(12) INTERNATIONAL APPLICATION PUBLISHED UNDER THE PATENT COOPERATION TREATY (PCT)

(19) World Intellectual Property Organization
International Bureau

(43) International Publication Date
28 March 2019 (28.03.2019)

WIPO | PCT

(10) International Publication Number
WO 2019/060795 A1

(51) International Patent Classification:
H01Q 15/10 (2006.01) *H01Q 21/06* (2006.01)

(21) International Application Number:
PCT/US2018/052321

(22) International Filing Date:
22 September 2018 (22.09.2018)

(25) Filing Language: English

(26) Publication Language: English

(30) Priority Data:
62/561,918 22 September 2017 (22.09.2017) US
62/562,547 25 September 2017 (25.09.2017) US
16/138,961 21 September 2018 (21.09.2018) US

(71) Applicant: **DUKE UNIVERSITY** [US/US]; 2018 Erwin Rd., Ste 306, Duke Box #90083, Durham, North Carolina 27705 (US).

(72) Inventors: **SMITH, David R.**; 5310 Sutteridge Ct., Durham, North Carolina 27713 (US). **SAPIRO, Guillermo**; 3 Acornridge Court, Durham, North Carolina 27707 (US). **MARKS, Daniel L.**; 4911 Centerway Drive, Durham, North Carolina 27705 (US). **BOWEN, Patrick**; 1206 Broad St., Durham, North Carolina 27705 (US). **ZECCA, Roberto**; 33 Forest Green Drive, Durham, North Carolina 27705 (US). **YURDUSEVEN, Okan**; 945 E. Mariposa St., Apt. 14, Altadena, California 91001 (US). **GOLLUB, Jonah N.**; 616 N. Queen St., Durham, North Carolina 27701 (US).

(74) Agent: **FLANAGAN, Justin K.**; 124 South 600 East, Salt Lake City, Utah 84102 (US).

(81) Designated States *(unless otherwise indicated, for every kind of national protection available)*: AE, AG, AL, AM, AO, AT, AU, AZ, BA, BB, BG, BH, BN, BR, BW, BY, BZ, CA, CH, CL, CN, CO, CR, CU, CZ, DE, DJ, DK, DM, DO, DZ, EC, EE, EG, ES, FI, GB, GD, GE, GH, GM, GT, HN,

(54) Title: SYMPHOTIC STRUCTURES

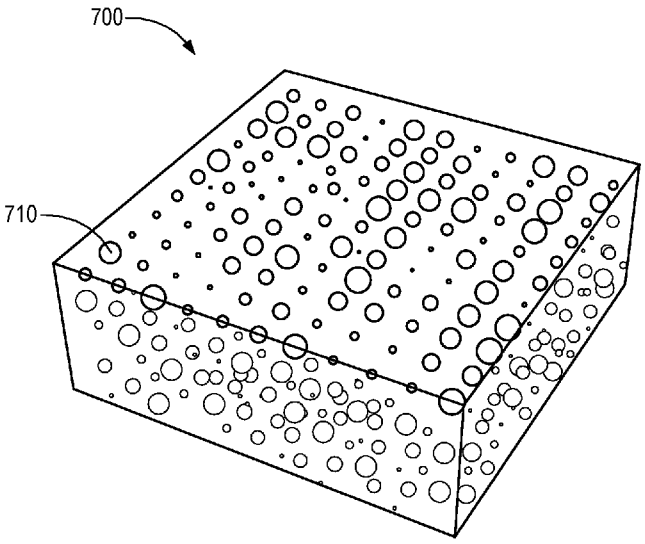


FIG. 7A

(57) Abstract: Systems and methods for designing, optimizing, patterning, forming, and manufacturing symphotic structures are described herein. A symphotic structure may be formed by identifying a continuous refractive index distribution calculated to convert each of a plurality of input reference waves to a corresponding plurality of output object waves. The continuous refractive index distribution can be modeled as a plurality of subwavelength voxels. The system can calculate a symphotic pattern as a three-dimensional array of discrete dipole values to functionally approximate the subwavelength voxels. A symphotic structure may be formed with a volumetric distribution of dipole structures. A dipole value, such as a dipole moment (direction and magnitude) of each dipole is selected for the volumetric distribution to convert a plurality of input reference waves to a target plurality of output object waves.

WO 2019/060795 A1

[Continued on next page]

HR, HU, ID, IL, IN, IR, IS, JO, JP, KE, KG, KH, KN, KP, KR, KW, KZ, LA, LC, LK, LR, LS, LU, LY, MA, MD, ME, MG, MK, MN, MW, MX, MY, MZ, NA, NG, NI, NO, NZ, OM, PA, PE, PG, PH, PL, PT, QA, RO, RS, RU, RW, SA, SC, SD, SE, SG, SK, SL, SM, ST, SV, SY, TH, TJ, TM, TN, TR, TT, TZ, UA, UG, US, UZ, VC, VN, ZA, ZM, ZW.

(84) **Designated States** *(unless otherwise indicated, for every kind of regional protection available)*: ARIPO (BW, GH, GM, KE, LR, LS, MW, MZ, NA, RW, SD, SL, ST, SZ, TZ, UG, ZM, ZW), Eurasian (AM, AZ, BY, KG, KZ, RU, TJ, TM), European (AL, AT, BE, BG, CH, CY, CZ, DE, DK, EE, ES, FI, FR, GB, GR, HR, HU, IE, IS, IT, LT, LU, LV, MC, MK, MT, NL, NO, PL, PT, RO, RS, SE, SI, SK, SM, TR), OAPI (BF, BJ, CF, CG, CI, CM, GA, GN, GQ, GW, KM, ML, MR, NE, SN, TD, TG).

Published:

— *with international search report (Art. 21(3))*

— *before the expiration of the time limit for amending the claims and to be republished in the event of receipt of amendments (Rule 48.2(h))*

Symphotic Structures

[0001] If an Application Data Sheet (ADS) has been filed on the filing date of this application, it is incorporated by reference herein. Any applications claimed on the ADS for priority under 35 U.S.C. §§ 119, 120, 121, or 365(c), and any and all parent, grandparent, great-grandparent, etc., applications of such applications are also incorporated by reference, including any priority claims made in those applications and any material incorporated by reference, to the extent such subject matter is not inconsistent herewith.

CROSS-REFERENCE TO RELATED APPLICATIONS

[0002] The present application claims the benefit of the earliest available effective filing date(s) from the following listed application(s) (the "Priority Applications"), if any, listed below (e.g., claims earliest available priority dates for other than provisional patent applications or claims benefits under 35 U.S.C. § 119(e) for provisional patent applications, for any and all parent, grandparent, great-grandparent, etc., applications of the Priority Application(s)). In addition, the present application is related to the "Related Applications," if any, listed below.

Priority Applications:

[0003] This application claims priority under 35 U.S.C. § 119(e) to U.S. Provisional Patent Application No. 62/561,918, filed on September 22, 2017, titled "Data-Driven Holographic Metamaterials for Optical Storage, Adaptive Objects and Acoustics", U.S. Provisional Patent Application No. 62/562,547, filed on September 25, 2017, titled "Data-Driven Holographic Metamaterials for Optical Storage, Adaptive Objects and Acoustics", and U.S. Non-Provisional Patent Application No. 15/138,961, filed on September 21, 2018, titled "Symphotic Structures," all of which are hereby incorporated by reference in their entireties. Moreover, all publications, texts, papers, appendices, and other materials cited within the above-identified provisional applications is hereby incorporated by reference, to the extent such subject matter is not inconsistent herewith.

Related Applications:

[0004] If the listings of applications provided above are inconsistent with the listings provided via an ADS, it is the intent of the Applicant to claim priority to each application that appears in the Priority Applications section of the ADS and to each application that appears in the Priority Applications section of this application.

[0005] All subject matter of the Priority Applications and the Related Applications and of any and all parent, grandparent, great-grandparent, etc., applications of the Priority

Applications and the Related Applications, including any priority claims, is incorporated herein by reference to the extent such subject matter is not inconsistent herewith.

TECHNICAL FIELD

[0006] This disclosure relates to volumetric index distributions for converting a set of input waves into a corresponding set of output waves. More specifically, this disclosure relates to static and reconfigurable finite three-dimensional arrays of conceptually polarizable subwavelength elements that can be optimized to functionally approximate continuous index distributions.

BRIEF DESCRIPTION OF THE DRAWINGS

[0007] Non-limiting and non-exhaustive embodiments of the disclosure are described herein, including various embodiments of the disclosure with reference to the figures listed below.

[0008] FIG. 1A illustrates a reference wave and an object wave interfering to create an interference pattern, according to one embodiment.

[0009] FIG. 1B illustrates the interference pattern in FIG. 1A used as the basis for determining an ideal hologram, according to one embodiment.

[0010] FIG. 2A illustrates a reference wave and an object wave interfering to create an interference pattern for determining an ideal hologram, according to one embodiment.

[0011] FIG. 2B illustrates an ideal hologram as a spatially varying refractive index distribution, according to one embodiment.

[0012] FIG. 2C illustrates the continuous, inhomogeneous material distribution of the ideal hologram discretized into a plurality of volume sub-elements, or voxels, according to one embodiment.

[0013] FIG. 2D illustrates the calculation of a symphotic pattern of dipole values that functionally approximates the volumetric subwavelength voxels, according to one embodiment.

[0014] FIG. 2E illustrates the ultimate realization of the symphotic pattern of dipole values formed as one or more metamaterial elements and/or dielectric particles, according to one embodiment.

[0015] FIG. 2F illustrates a three-dimensional representation of a continuous, inhomogeneous material distribution for a finite aperture ideal hologram.

[0016] FIG. 2G illustrates the finite aperture ideal hologram modeled as a plurality of subwavelength homogenous voxels, according to one embodiment.

[0017] FIG. 3 illustrates a simple model of an electrical dipole with the magnitude and direction of the dipole moment vector represented by an arrow, according to one embodiment.

[0018] FIG. 4A illustrates a non-resonant electric I-Beam dipole, according to one embodiment.

[0019] FIG. 4B illustrates an example of a split ring resonator (SRR) magnetic dipole, according to one embodiment.

[0020] FIG. 4C illustrates a resonant electric inductor-capacitor (ECL) resonator, according to one embodiment.

[0021] FIG. 5A illustrates a model of a high dielectric nanoparticle exhibiting a Mie as an electric dipole, according to one embodiment.

[0022] FIG. 5B illustrates a model of a magnetic dipole, according to one embodiment.

[0023] FIG. 5C illustrates the scattering cross-section of the high dielectric nanoparticles as electric and magnetic dipoles, according to one embodiment.

[0024] FIG. 6 illustrates several materials that can be used to fabricate symphotic structures, spectral ranges, and refractive indices, according to one embodiment.

[0025] FIG. 7A illustrates a symphotic structure formed as a three-dimensional array of high-dielectric sphere dipole elements, according to one embodiment.

[0026] FIG. 7B illustrates a symphotic structure formed via a multi-layer manufacturing approach for infrared and visible wavelength operation, according to one embodiment.

[0027] FIG. 8 illustrates a graph of dielectric TiO2 spheres with a 75-nm radius to show that, with large distances, the extracted polarizability conforms to a single sphere using Mie theory, according to one embodiment.

[0028] FIG. 9 illustrates a symphotic structure formed as a three-dimensional array of high-dielectric sphere dipole elements according to one embodiment.

[0029] FIG. 10 illustrates a well-aligned structure demonstrating the feasibility of manufacturing small-scale dipole elements in a highly accurate matrix, according to one embodiment.

[0030] FIG. 11 illustrates an array of metamaterial elements as polarizable dipoles to form a symphotic structure with bias lines that can be used to modify one or more dipole values to reconfigure the symphotic structure, according to one embodiment.

[0031] FIG. 12 illustrates a characteristic example of an acoustic metamaterial utilized to make a ground cloak.

DETAILED DESCRIPTION

[0032] This disclosure includes various systems, apparatuses, and methods that relate to modeling, optimizing, constructing, and dynamically tuning functional approximations of continuous volumetric index distributions for converting a set of input waves into a set of output waves. This disclosure builds on the basic understanding that a volumetric index distribution can produce a set of distinct output spatial wave patterns in response to a set of input waves that vary in incidence angle and/or frequency. The material(s) selection for the volumetric structure depends on the desired bandwidth and wave type.

[0033] For example, a volumetric distribution of dielectric resonators can provide a strong scattering response with minimal resistive losses for infrared and visible wavelengths of electromagnetic radiation. In contrast, metallic resonators may be suitable for spatial wave conversion at lower electromagnetic frequencies, such as microwave and millimeter wave frequencies. In fact, volumetric distributions of materials having various bulk moduli and densities can be used to convert a set of input acoustic waves to a determinable set of output acoustic waves. Structures may be generated with specific volumetric index distributions to enable highly parallelizable and ultrafast spatial wave processing. Systems and methods are described herein for designing, optimizing, and forming symphotic structures that include volumetric distributions of dipole structures. The interelement spacings may be subwavelength and a dipole value of each dipole structure may be selected so as to convert a plurality of input reference waves to a target plurality of output object waves.

[0034] Examples of discrete dipole approximations and modeling are described in U.S. Patent Publication 2016/0204515 filed by Yi, titled “Discrete-Dipole Methods and Systems For Applications To Complementary Metamaterials,” which is hereby incorporated by reference in its entirety. Various metamaterials and foundational principles thereof are described in U.S. Patent 8,040,586 filed by Ben, titled “Metamaterials,” which is hereby incorporated by reference in its entirety. Scattering elements suitable for use by the presently described system and methods can include complementary metamaterial elements such as those presented in D. R. Smith et al, "Metamaterials for Surfaces and Waveguides," U.S. Patent Application Publication No. 2010/0156573, and A. Bily et al, "Surface Scattering Antennas," U.S. Patent Application Publication No. 2012/0194399, each of which is hereby incorporated by reference. Similarly, the scattering elements can include patch elements such as those presented in A. Bily et al, "Surface Scattering Antenna Improvements," U.S. United States Patent Application No. 13/838,934, which is hereby incorporated by reference.

[0035] Surface scattering antennas that include a waveguide coupled to a plurality of subwavelength patch elements are described in U.S. Patent Application Publication No. 2014/0266946. Surface scattering antennas that include a waveguide coupled to adjustable scattering elements loaded with lumped/active devices are described in U.S. Application Publication No. 2015/0318618. Surface scattering antennas that feature a curved surface are described in U.S. Patent Application Publication No. 2015/0318620. Surface scattering antennas that include a waveguide coupled to a plurality of adjustably-loaded slots are described in U.S. Patent Application Publication No. 2015/0380828. And various holographic modulation pattern approaches for surface scattering antennas are described in U.S. Patent Application Publication No. 2015/0372389. All of these patent applications include systems, methods, devices, approaches, and foundational material that can be used to form the symphotic structure described herein, and each of the above-identified patent references is hereby incorporated by reference in its entirety.

[0036] Finally, U.S. Patent Pub. No. 2018/0241131 titled "Optical Surface Scattering Antennas" and all other patent applications claiming priority thereto or to which this publication claims priority are hereby incorporated by reference in their entireties. These applications discuss surface holographic technology involving a surface that is populated with a plurality of adjustable optical resonators. In some embodiments, symphotic structures, as described herein, may be implemented using adjustable optical resonators such as those described in these references.

[0037] The field of holography is related to the presently described systems and methods. In fact, many of the proposed solutions, applications, benefits, materials, and computational approaches developed for holography are applicable to the systems and methods described herein. However, holographic approaches for controlling waves rely on programming, calculating, or approximating an interference pattern. The holographic solution to converting an input wave to target output wave constitutes constructing an index modulation pattern that matches the interference pattern produced by the combination of the input wave and the target output wave.

[0038] In the ideal case, a volume hologram can convert a set of input waves into a set of output waves. Unfortunately, this is only true when the incident wave is unperturbed. Because volume holographs are conceptually modeled as interference patterns known, programmed, or even recorded to vary the phase and amplitude of a reference input wave, the output wave is inherently depleted as it passes through the volume. These inefficiencies are compounded even further for large-magnitude index variations. Thus, while holography works well for surface

holograms, the practical limitations and inefficiencies associated with volume interference patterns render holographic approaches to volumetric spatial wave conversion inadequate. This disclosure proposes a departure from the traditional holographic approach based on interference patterns.

[0039] In its place, volumetric structures are proposed in which finite arrays of conceptually polarizable dipoles are mathematically modeled as functional equivalents to continuous index distributions. The term "symphotic" is used throughout this disclosure to refer to a wide variety of finite-array approximations of continuous index distributions, including those modeled as three-dimensional arrays of discrete dipole values. The term "symphotic pattern" can be used to describe a calculated three-dimensional array of discrete dipole values that functionally approximates a more continuous material or material having a higher order of selectivity. The concept of a "symphotic pattern" may also be applied to a two-dimensional array of conceptually polarizable dipoles that functionally approximates a surface hologram or other surface distribution of index material, but this disclosure focuses primarily on three-dimensional symphotic patterns and the formation of three-dimensional, or volumetric, symphotic structures.

[0040] To provide a specific example, a symphotic structure may be formed by depositing, printing, etching, or otherwise manufacturing a physical array of dipole elements having static or dynamically tunable dipole values as specified by a three-dimensional symphotic pattern. The development and calculation of the symphotic pattern may begin with the identification of a continuous refractive index distribution calculated or measured to convert each of a plurality of input reference waves to a corresponding plurality of output object waves. By virtue of converting a plurality of input reference waves to a corresponding plurality of output object waves, it is implied that this continuous refractive index distribution is volumetric and inhomogeneous.

[0041] The distribution of dielectric constants and the materials used in the volume may be idealized as a graded-permittivity structure having a continuous distribution of dielectric constants, such that there are no abrupt changes in permittivity across the structure. Assuming finite operational bandwidth, a discretized piecewise-continuous approximation of the graded-permittivity structure may be electromagnetically equivalent.

[0042] Accordingly, inhomogeneous continuous refractive index distribution is modeled as a plurality of discretized, homogeneous volumes, referred to as "voxels," that have subwavelength dimensions. An optimization problem attempting to solve for the values and properties of a continuously variable refractive index material may be intractable unless some

approximations are made. Even after reducing the number of variables for optimization to a discrete number of homogeneous voxels, solving for the index distribution still amounts to a difficult inverse problem with many variables.

[0043] However, by considering a three-dimensional array of discrete dipole values as functionally approximating the subwavelength voxels, the number of unknowns is significantly reduced, and the entire optimization problem can be tractably computed with modest processing resources.

[0044] In various embodiments, a symphotic structure to convert electromagnetic input reference waves into output object waves may include a three-dimensional array of discrete dipole elements with subwavelength interelement spacings, and may be practically realized through any of a wide variety of approaches, including, without limitation, through the use of high-dielectric nanoparticles, plasmonic nanoparticles, and other polarizable dipoles that, for a given operational bandwidth, can be configured in an array with subwavelength interelement spacings.

[0045] In various embodiments, metamaterial dipoles may be utilized to provide a wide range of synthetic control within specific operational bandwidths. The interacting dipole model serves as the framework for the simulation and optimization of optically large, volumetric structures. The specific materials, dimensions, and reconfigurability may depend on the target functionality.

[0046] For example, volumetric acoustic metamaterials can be engineered with a similar approach to those discussed above, but with consideration for bulk modulus and density variables instead of electromagnetic properties of permittivity and the like. For embodiments in which the acoustic waves will ultimately propagate in the air, the optimization analysis can be further restricted to compression waves and make use of a scalar wave equation. Moreover, the acoustic equivalent of the symphotic patterns for electromagnetic embodiments may be expressed as scattered fields of discrete acoustic monopoles, which can be optimized for a desired field structure. With the understanding that acoustic versions of nearly every embodiment are possible, the remainder of this disclosure focuses primarily on electromagnetic embodiments to avoid unnecessary duplication.

[0047] One advantage of the symphotic design approach described herein is that by considering a medium of dipoles from the outset, the number of variables for optimization remains easily computable. In fact, as discussed below in greater detail, the optimization problem may be computed sufficiently quickly to allow for locally reconfigurable symphotic structures that can be dynamically tuned in real time.

[0048] As previously described, an initial continuous index distribution may be identified as the basis for ultimately calculating the discrete dipole values. The initial continuous index distribution may be identified in a number of ways depending on the target functionality. The traditional interference approach can be used to identify an initial continuous index distribution and is used in the example below with reference to FIGS. 1A-2E.

[0049] FIG. 1A illustrates a reference wave 102 and an object wave 104 interfering to create an interference pattern 106.

[0050] FIG. 1B illustrates the interference pattern 106 in FIG. 1A being used as the basis for determining an ideal hologram 110. It is appreciated that this simple approach can be greatly expanded for multiplex volume holograms and could be accomplished via computer simulation or mathematical computation.

[0051] FIG. 2A is repetitive of FIGS. 1A and 1B, but is reproduced on the same drawing sheet as FIGS. 2B-2E for continuity and understanding. Specifically, FIG. 2A illustrates a reference wave 202 and an object wave 204 interfering to identify parameters for an ideal hologram 210 that can be subsequently used to convert the reference wave 202 into the object wave 204.

[0052] FIG. 2B illustrates ideal hologram 210 as a spatially varying refractive index distribution or variation in other material parameter (e.g, density or bulk modulus for acoustic embodiments).

[0053] FIG. 2C illustrates the continuous, inhomogeneous material distribution of the ideal hologram 210 discretized into a plurality of volume sub-elements, or voxels 215, each of which is approximated as a homogeneous material. The workflow in FIGS. 2A-2E shows a two-dimensional representation of the discretization; however, the discretization of the continuous inhomogeneous material 210 into homogeneous voxels 215 occurs in all three dimensions.

[0054] FIG. 2F illustrates a three-dimensional representation of a continuous, inhomogeneous material distribution for a finite aperture ideal hologram 210.

[0055] FIG. 2G illustrates the finite aperture ideal hologram 210 of FIG. 2F modeled as a plurality of subwavelength voxels 215, each of which is homogenous and collectively approximate the ideal hologram 210 of FIG. 2F. It can be conceptually understood that if the "boxes" representing individual voxels 215 were small enough, FIG. 2G would be visually indistinct from FIG. 2F. In a conceptually analogous way, by modeling the voxels 215 to have subwavelength dimensions for the operational bandwidth, frequencies within that bandwidth will have indistinguishable responses to the continuous inhomogeneous material 210 of FIG. 2F and plurality of subwavelength voxels 215.

[0056] In various embodiments, a combination of voxel shapes and/or sizes may be used. Moreover, voxels may be shaped and/or sized such that little or no space, gaps, or voids exist between voxels. Alternatively, voxels may be arranged such that gaps or voids of various sizes and/or shapes exist intentionally. In some embodiments, the gaps or voids may be ignored and/or negligible in calculating the volumetric dielectric constants. Alternatively, the gaps or voids may be assigned one or more dielectric constants corresponding to a vacuum or to air or another fluid that fills the gaps or voids. In some embodiments, the voxels may be cubes, parallelepipeds, tetrahedrons, prisms, various regular polyhedrons, or other polyhedrons.

[0057] The holographic lens may be conceptually discretized to facilitate the use of optimization algorithms, examples of which are described herein and can be found in U.S. Patent Application No. 14/638,961 filed on March 4, 2015, titled "Holographic Mode Conversion for Electromagnetic Radiation," which application and all applications that claim priority thereto are hereby incorporated by reference in their entireties.

[0058] FIG. 2D illustrates the calculation of a symphotic pattern of dipole values that functionally approximates the volumetric subwavelength voxels 215. Again, FIG. 2D illustrates a single two-dimensional layer of the symphotic pattern of dipole values. The symphotic pattern may be calculated as a three-dimensional array of discrete dipole values. The three-dimensional array of discrete dipole values functionally approximates the plurality of subwavelength voxels 215, which in turn model the continuous refractive index distribution of the ideal hologram 210.

[0059] FIG. 2E illustrates the ultimate realization of the symphotic pattern of dipole values as a variety of metamaterial elements and/or dielectric particles of various sizes.

[0060] Within the framework of the interacting dipole model, various optimization approaches can be leveraged to improve the functionality, simplify manufacturing, reduce the number of unique dipole elements, or achieve another optimization target. In some embodiments, optimization approaches can leverage advanced machine learning and functional approximation methods.

[0061] The individual dipole values for a given symphotic mapping of input waves to output waves is locally computable. Accordingly, a local dynamically reconfigurable volumetric symphotic structure can be created by adding the ability to modify one or more properties of individual dipoles, small groups of dipoles, rows of dipoles, or clusters of dipoles. For example, one or more external voltage controls may be added to a volumetric distribution of magnetic and/or electric dipole elements that allows each dipole element to be individually adjusted. For example, each external control signal may allow for manipulation of the magnitude and/or

direction of the dipole moment of one or more of the dipoles. In some embodiments, external control signals may be arranged to provide addressability of individual or groups of dipoles for individual or collective tuning.

[0062] FIG. 3 illustrates a simple model of an electrical dipole with the magnitude and direction of the dipole moment vector represented by the arrow 310. At low frequencies, electrical dipoles form in any conducting or dielectric particle (i.e. any structure that produces a charge separation in response to applied field). Dipole responses dominate electrically small objects, with respect to wavelength.

[0063] FIG. 4A illustrates a non-resonant electric I-Beam dipole, according to one embodiment.

[0064] FIG. 4B illustrates an example of a split ring resonator (SRR) magnetic dipole, according to one embodiment.

[0065] FIG. 4C illustrates a resonant electric inductor-capacitor (ECL) resonator, according to one embodiment.

[0066] FIG. 5A illustrates a model of a high dielectric nanoparticle exhibiting a Mie as an electric dipole, according to one embodiment. The legend in FIG. 5B is applicable to FIG. 5A as well.

[0067] FIG. 5B illustrates a model of a magnetic dipole, according to one embodiment.

[0068] FIG. 5C illustrates the scattering cross-section of the electric and magnetic dipoles at various wavelengths. High dielectric nanoparticles support optical, or Mie, resonances which behave like polarizable electric magnetic dipoles. As illustrated by the scattering at various wavelengths, it can be readily appreciated that such particles may be used in forming the symphotic structure of dipole elements.

[0069] FIG. 6 illustrates several materials, spectral ranges, and refractive indices. Each of these materials may be used as part of a symphotic structure, depending on the specific bandwidth and target functionality of the symphotic structure.

[0070] The advantages and applications of locally reconfigurable volumetric index materials, especially those utilizing dielectric index materials for operation in optical or quasi-optical bandwidths, are widely recognized and discussed in the context of related fields, such as volumetric holography. The presently described locally reconfigurable symphotic structure functionally approximates true inhomogeneous volumetric index distributions and can therefore provide all the desired functionality for any and/or all of these applications. For example, various embodiments and adaptations of the static and/or reconfigurable symphotic structures described herein may be used as/in/for: dynamic holographic memory,

mode-matching devices, imaging, machine vision, physical layer pattern recognition, optical mode conversion, chemical detection, coherence measurements, filtering, interferometry, data storage, multiport storage, multiplexed dense storage, holonomic brain type architectures, neuroscience applications, ultrafast and precise analog-to-digital converters, communication multiports, image processing, signal processing, ultrafast search modes, encryption and security applications, and any other application requiring ultrafast linear processing or parallel processing.

[0071] The specific configuration, size, bandwidth, wave conversion, and other properties of symphotic structures may vary based on the intended usage. Regardless of the particular application, a continuous refractive index distribution can be identified to provide for the conversion of a set of input waves to be converted to a set of output waves. As previously noted, a holographic approach based on interference patterns may be used to define the initial volumetric index distribution. In other embodiments, any of the numerous approaches known in the field may be utilized. For example, a linear solution based on a variation approach may be used, as described in *Marks, Daniel L. and Smith, David R, 2018, Linear Solutions to Metamaterial Volume Hologram Design Using a Variational Approach, Journal of the Optical Society of America, 35(4):567-76*, which publication is hereby incorporated by reference in its entirety.

[0072] In many, if not all, practical applications, an identified volumetric index distribution cannot be manufactured as ideally specified. An implementation step is applied to reduce the continuous material distribution to a manufacturable material and/or metamaterial. For example, an ideal holographic design can be expressed as a dielectric function $\varepsilon(\mathbf{r})$, and the relationship between the reference field $UR(\mathbf{r})$ and the scattered field $US(\mathbf{r})$ in the first Born approximation is:

[0073] $$\nabla 2US+\varepsilon 0\omega 2c2US=-(\varepsilon(\mathbf{r})-\varepsilon 0)\omega 2c2UR=-\varepsilon 0\chi(\mathbf{r})\omega 2c2UR=-\omega 2c2P(\mathbf{r}) \quad EQ.\ 1$$

[0074] In EQ. 1, $\varepsilon 0$ is the permittivity of free space, $\varepsilon(\mathbf{r})$ is the spatially varying dielectric function of the material, c is the speed of light in vacuum, and ω is the angular frequency of the wave. The permittivity can be expressed in terms of the medium susceptibility, $\chi(\mathbf{r})$, which—when multiplied by the reference field—can be written as a continuous polarization field, $P(\mathbf{r})$.

[0075] The example provided herein assumes that the waves are scalar, but the algorithms can be readily extended to vectorial formulations as would be applicable to various embodiments of the systems and methods described herein. Sampling the material at discrete

points and using the free space propagator, the scattered field in terms of the reference field (up to a constant) can be expressed as:

[0076] $US(\mathbf{r}i)=\Sigma G(\mathbf{r}'i,\mathbf{r}j)Pjj=\Sigma G(\mathbf{r}'i,\mathbf{r}j)pjVj=\Sigma G(\mathbf{r}'i,\mathbf{r}j)\alpha jVUR(\mathbf{r}j)j$ *EQ. 2*

[0077] The free space propagator has the form $G(\mathbf{r}'i,\mathbf{r}j)\sim\exp(ik0|\mathbf{r}'i-\mathbf{r}j|)/|\mathbf{r}'i-\mathbf{r}j|$. Here, the continuous polarizability function has been transformed to point dipoles, each with a polarizability αj. EQ. 2 expresses the scattered field as a sum of dipole (j) contributions. Each dipole moment is determined by the polarizability, αj, multiplied by the reference field at the location, $\mathbf{r}j$. Consistent with the homogenous voxel modeling shown in FIG. 2C, the local dielectric function is a constant over each local volume. Accordingly, the polarizability is represented by VPj. Values for the αj can be determined quite accurately using, for example, effective medium theory. However, the dipole interactions can be self-consistently taken into account, and the local dipole moments can be found to a better approximation using an improved form of the discrete dipole approximation as follows:

[0078] $\alpha i-1\Sigma[\delta ij-\alpha iG(\mathbf{r}i,\mathbf{r}j)]pj=UR(\mathbf{r}i)$

EQ. 3

[0079] The dipole moments identified using EQ. 3 can be used with EQ. 2 to calculate a more accurate approximation to the scattered field for dipole-based functional approximations. Any of a wide variety of optimization, functional approximation, and machine-learning techniques may utilize a form, model, or similariton of EQ. 2 to improve on an initial volumetric index distribution. The optimization systems and algorithms may be designed to improve the accuracy of the mapping of input reference waves to output object waves, improve operational efficiency, and/or reduce the complexity of manufacturing.

[0080] The optimizations may be specifically configured to optimize for dipole-based functional approximations of volumetric index distributions initially identified using, for example, holographic interference techniques, coupled mode theory, and/or linear or multiplex variational approaches. The set of polarizabilities can be used as optimization variables and altered to achieve the best values for a target set of input and output waves. The systems and methods described herein facilitate large-scale optimization, which serves as the basis for a comprehensive volumetric design approach with a reduced solution space.

[0081] In various embodiments, advancements in machine learning can be leveraged to improve the initial design and/or formation of a symphotic structure. In other embodiments,

machine learning techniques can be used for manipulating control signals of dynamically reconfigurable symphotic structures.

[0082] A three-dimensional array of dipole elements may be formed (e.g., manufactured, printed, etched, etc.) for microwave and millimeter wave frequencies using a wide variety of available resonant and non-resonant dipoles, including various metamaterial dipoles such as the I-beam, SSR and ELC dipoles exemplified in FIGS. 4A-C.

[0083] FIG. 7A illustrates a symphotic structure 700 formed as a three-dimensional array of high-dielectric sphere dipole elements 710. The dipole elements 710 may have various dipole values, such as dipole moments, that are represented by the different-sized spheres. The dipole elements 710 are maintained in the three-dimensional array by a low dielectric host material.

[0084] FIG. 7B illustrates a symphotic structure 750 (potentially a functional equivalent of symphotic structure 700 in FIG. 7A) formed via a multi-layer 720-725 manufacturing approach. At infrared and visible wavelengths, dielectric resonators, such as the spheres illustrated in FIGS. 7A and 7B, may be selected to form the symphotic structure because they provide a strong scattering response with minimal resistive losses. Symphotic structures may be formed using layer stacking and/or three-dimensional printing.

[0085] A variety of high dielectric materials with varying properties can be used for optical metamaterials. For example, TiO2, GaP, Te, PbTe, SiC and many other materials can be extremely low-loss over specific bands in the visible or infrared range. Using dielectric particles or various metamaterial elements, the intrinsic polarizability can be determined by computing the scattering coefficients for a single, infinitely periodic lattice of identical elements, and then applying an effective medium theory.

[0086] In FIG. 8, dielectric TiO2 spheres with a 75-nm radius are graphed 750 to show that if distance between the spheres is large enough (>0.1 x the radius), the extracted polarizability agrees with that of a single sphere using Mie theory. Using polarizability extraction, an equivalent and accurate dipole description of a collection of metamaterial elements can be applied and used as a computational tool for largescale iterative optimization cycles.

[0087] Another advantage of the symphotic approaches described herein is that the dipole formalism is compatible with parallelization, so that graphic processing units (GPUs) can be leveraged for fast and efficient modeling.

[0088] In some embodiments and applications, the overall size of the symphotic structure may be suitable for various emerging fabrication techniques, such as planar fabrication methods combined with stacking and multilayer metamaterial structures. Similarly, techniques

such as planar optics for infrared bands and techniques for addressing issues of alignment and integration may also facilitate the formation of symphotic structures. The planar fabrication technique may facilitate the formation of reconfigurable symphotic structures because of the electrical lead structures that facilitate the application of tunable bias voltages or other stimuli. Many of these structures can be fabricated on low dielectric substrates (with transparent leads for reconfigurable samples), then bonded together to form the final symphotic structure.

[0089] FIG. 9 illustrates a symphotic structure 900 formed as a three-dimensional array of high-dielectric sphere dipole elements 910. The dipole elements 910 may have various dipole moments, that are represented by the different-sized spheres. The dipole elements 910 are maintained in the three-dimensional array by a low dielectric host material manufactured on top of a substrate 925.

[0090] FIG. 10 illustrates a well-aligned structure 1000 demonstrating the feasibility of manufacturing small-scale dipole elements in a highly accurate matrix, according to one embodiment.

[0091] Reconfigurable symphotic structures may be formed using components like SRRs, ELCs, and the like that are loaded with PIN diodes, varactors, or other tunable or variable-bias type devices. In some embodiments, liquid crystal may be employed to dynamically affect the polarization values of one or more dipole elements in a three-dimensional array of dipole elements.

[0092] FIG. 11 illustrates an array of metamaterial elements 1100 as polarizable dipoles to form a symphotic structure with bias lines 1105 that can be used to modify one or more dipole values to reconfigure the symphotic structure. The illustrated embodiment is suitable for operation in microwave bandwidths and may include varactor-loaded metamaterial resonators driven by the bias lines.

[0093] As previously noted, although the mathematical equations and specific examples above were generally described in the context of electromagnetic radiation embodiments utilizing electrical and/or magnetic dipoles, it is appreciated that volumetric acoustic metamaterials can be engineered with a similar design approach to modify pressure fields of, for example, ultrasonic or audible compression waves.

[0094] FIG. 12 illustrates a characteristic example of an acoustic metamaterial utilized to make a ground cloak. In some acoustic embodiments, the initial volumetric index distribution may be specified as a distribution of acoustic materials with various acoustic properties, such as linear and dynamic density tensor properties, bulk modulus, elastic modulus, density, or

other acoustic property. An initial volumetric distribution of acoustic refractive indices may be found to satisfy the following expression:

[0095] $$n^2(x,y,z) - 1 = C\,\boldsymbol{p}_{in} \cdot \boldsymbol{p}^*_{goal} / \left|\boldsymbol{p}_{goal}\right|^2 \qquad EQ.\ 4$$

Where $n(x,y,z)$ is the volumetric distribution of acoustic refractive indices, β is a selectable normalization constant, $\boldsymbol{P}_{in}$ is the input acoustic pressure field distribution, $\boldsymbol{p}_{goal}$ is the output pressure field distribution.

[0096] In various embodiments, acoustic symphotic structures may be based on acoustic dipole and/or monopole responses. Some embodiments may utilize tunable acoustic metamaterials, such as piezoelectric components, to allow for dynamic reconfigurability.

[0097] Any of a wide variety of materials and methods of manufacturing may be employed. For example, a symphotic structure may be manufactured, at least in part, using glass-forming materials, polymers, metamaterials, aperiodic photonic crystals, silica, composite metamaterials, porous materials, foam materials, layered composite materials, stratified composite materials, fiber-bundle materials, micro-rod materials, nano-rod materials, a non-superluminal low-loss dielectric material, porcelain, glass, plastic, air, nitrogen, sulfur hexafluoride, parylene, mineral oil, ceramic, paper, mica, polyethylene, and/or aluminum oxide.

[0098] A symphotic structure may be used as a distributed storage, an optical lens, an acoustic converter, and a three-dimensional imaging device. A symphotic structure may be configured for use as one of: a hyperspectral imaging device, encryption algorithms, machine vision, distributed learning, and chemical detection. A symphotic structure may be used as an imaging sensor to receive the output object waves as processed image information, convert electromagnetic input reference waves to electromagnetic output object waves, convert optical input reference waves to optical output object waves, convert infrared input reference waves to infrared output object waves, and/or to convert visible light input reference waves to visible light output object waves.

[0099] The symphotic structures may be configured for operation with RF, microwaves, terahertz, millimeter-waves, acoustic output waves, and/or ultrasonic waves. The symphotic structures may be configured to upconvert or downconvert the frequency of reference waves. The symphotic structures may be configured to convert audible input reference waves to audible output object waves, convert audible input reference waves from first and second audio channels to audible output object waves directed to different spatial locations, and/or convert

acoustic input reference waves from each of a plurality of audio channels to audible output object waves that are spatially localized and fully isolated from one another.

[00100] A symphotic structure may include dipole structures configured to output a unique object wave for each unique frequency of input wave, each unique angle of incidence of input wave, and/or each unique angle of incidence and frequency of input wave. A symphotic structure may have a static value to provide for a static conversion of input reference waves to output object waves or include control signals to dynamically tune at least some of the dipole structures. The control signals may be coupled to one of a varactor and a PIN diode, useable to select a polarization value of each dipole structure.

[00101] Some of the dipole elements are tunable by one or more of electrically controllable liquid crystals, varactors, PIN diodes, MEMs, ferroelectrics, physical deformation, and mechanical actuation. At least some of the dipole structures may comprise electric I-beam LC dipole elements or be tuned via elements having a capacitance and an inductance. At least some of the dipole structures may comprise metamaterial electric I-beam LC dipole elements.

[00102] A symphotic structure may comprise magnetic resonators for converting electromagnetic input reference waves to electromagnetic output object waves, such as split ring resonators (SRRs) and electric inductor-capacitor resonators (ELCs). The dipole structures comprise metamaterial dielectric resonators for conversion of optical electromagnetic input reference waves to optical electromagnetic output object waves. The metamaterial dielectric resonators may comprise nanoparticles with fixed Mie resonances, nanoparticles with tunable Mie resonances, and/or a set of metamaterial dielectric spheres in a three-dimensional array.

[00103] The metamaterial dielectric spheres in the three-dimensional array may be set within a lower dielectric host background. The metamaterial dielectric resonators may comprise one or more of: TiO_2, GaP, Te, PbTe, and SiC.

[00104] Intrinsic polarizability of the metamaterial dielectric resonators may be computed based on an effective medium theory of scattering coefficients of a single, infinitely periodic lattice of identical elements. At least some of the dipole structures may comprise dielectric resonators for conversion of optical electromagnetic input reference waves to optical electromagnetic output object waves. The dielectric resonators may comprise nanoparticles with fixed Mie resonances, nanoparticles with tunable Mie resonances, and/or a set of dielectric spheres in a three-dimensional array. The dielectric spheres in the three-dimensional array may be set within a lower dielectric host background.

[00105] A symphotic structure may have dipole structures configured to convert M unique input reference waves to N unique output object waves, where M and N are positive integers, wherein M is equal to N, M is greater than N, or M is smaller than N.

[00106] A symphotic structure may include an array of varactor-loaded resonators in communication with the dipole structures and bias lines for driving the varactors for dynamic reconfiguration of the three-dimensional array. The varactor-loaded resonators may be embodied as metamaterials.

[00107] Aspects of the invention are set forth in the following numbered clauses:

1. A method of forming a symphotic structure, comprising:

identifying a continuous refractive index distribution to convert each of a plurality of input reference waves to a corresponding plurality of output object waves;

modeling the continuous refractive index distribution as a plurality of subwavelength voxels;

calculating a three-dimensional array of discrete dipole values (a "symphotic pattern") to functionally approximate the subwavelength voxels; and

forming the symphotic pattern of dipole values as a three-dimensional array of dipole elements to convert the plurality of input reference waves to the corresponding plurality of output object waves.

2. The method of aspect 1, wherein the three-dimensional array of dipole elements is configured to convert electromagnetic input reference waves to electromagnetic output object waves.

3. The method of aspect 2, wherein the three-dimensional array of dipole elements is configured to convert optical input reference waves to optical output object waves.

4. The method of aspect 3, wherein the three-dimensional array of dipole elements is configured to convert infrared input reference waves to infrared output object waves.

5. The method of aspect 3, wherein the three-dimensional array of dipole elements is configured to convert visible light input reference waves to visible light output object waves.

6. The method of aspect 2, wherein the dipole structures are configured to convert microwave input reference waves to microwave output object waves.

7. The method of aspect 2, wherein the dipole structures are configured to convert terahertz input reference waves to terahertz output object waves.

8. The method of aspect 2, wherein the dipole structures are configured to convert millimeter-wave (MMW) input reference waves to MMW output object waves.

9. The method of aspect 2, wherein the three-dimensional array of dipole elements is configured to convert radio frequency (RF) input reference waves to RF output object waves.

10. The method of aspect 9, wherein the three-dimensional array of dipole elements is configured to upconvert the frequency of the RF output object waves relative to the RF input reference waves.

11. The method of aspect 9, wherein the three-dimensional array of dipole elements is configured to downconvert the frequency of the RF output object waves relative to the RF input reference waves.

12. The method of aspect 9, wherein the three-dimensional array of dipole elements is configured to operate in a 77 GHz bandwidth.

13. The method of aspect 1, wherein at least some of the dipole elements comprise metamaterial dipole elements.

14. The method of aspect 1, wherein the three-dimensional array of dipole elements is configured to convert acoustic input reference waves to acoustic output object waves.

15. The method of aspect 14, wherein the three-dimensional array of dipole elements is configured to convert ultrasonic input reference waves to ultrasonic output object waves.

16. The method of aspect 14, wherein the three-dimensional array of dipole elements is configured to upconvert the frequency of the acoustic output object waves relative to the acoustic input reference waves.

17. The method of aspect 14, wherein the three-dimensional array of dipole elements is configured to downconvert the frequency of the acoustic output object waves relative to the acoustic reference waves.

18. The method of aspect 14, wherein the three-dimensional array of dipole elements is configured to convert audible input reference waves to audible output object waves.

19. The method of aspect 18, wherein the three-dimensional array of dipole elements is configured to convert audible input reference waves from first and second audio channels to audible output object waves directed to different spatial locations.

20. The method of aspect 14, wherein the three-dimensional array of dipole elements is configured to convert the acoustic input reference waves from each of a plurality of audio channels to audible output object waves that are spatially localized and fully isolated from one another.

21. The method of aspect 1, wherein the continuous refractive index distribution comprises a continuous distribution of permittivity values.

22. The method of aspect 1, wherein each subwavelength voxel is defined to have a homogenous refractive index.

23. The method of aspect 1, each of the subwavelength voxels is represented as a

polarization state.

24. The method of aspect 1, each of the subwavelength voxels is represented as a homogeneous permittivity.

25. The method of aspect 1, wherein the continuous refractive index distribution comprises a continuous distribution of bulk modulus and density values.

26. The method of aspect 1, each of the subwavelength voxels is represented as a homogeneous bulk modulus value and density value.

27. The method of aspect 1, wherein each of the plurality of input reference waves is defined in terms of frequency, and where the three-dimensional array of dipole elements is configured to output a unique object wave for each unique frequency of input wave.

28. The method of aspect 1, wherein each of the plurality of input reference waves is defined in terms of angle of incidence, such that the three-dimensional array of dipole elements to is configured to output a unique object wave for each unique angle of incidence of input wave.

29. The method of aspect 1, wherein each of the plurality of input reference waves is defined in terms of frequency and angle of incidence, such that the three-dimensional array of dipole elements to is configured to output a unique object wave for each unique angle of incidence and frequency of input wave.

30. The method of aspect 1, wherein each of the dipole elements in the three-dimensional array has a static value to provide for a static conversion of input reference waves to output object waves.

31. The method of aspect 1, wherein at least some of the dipole elements in the three-dimensional array are dynamically tunable via a plurality of control signals.

32. The method of aspect 31, further comprising:

dynamically modifying at least one of the plurality of control signals to modify the conversion of input reference waves to output object waves.

33. The method of aspect 31, wherein each of the dipole elements is coupled to one of a varactor and a PIN diode, wherein each of the plurality of control signals is useable to select a polarization value of each dipole element.

34. The method of aspect 31, wherein at least some of the dipole elements are tunable by at least one of: electrically controllable liquid crystals, varactors, PIN diodes, MEMs, ferroelectrics, physical deformation, and mechanical actuation.

35. The method of aspect 31, wherein at least some of the dipole elements are tunable via

electrical biases.

36. The method of aspect 31, further comprising:

identifying a second continuous refractive index distribution to convert each of the plurality of input reference waves to a different set of output object waves;

modeling the second continuous refractive index distribution as a second set of subwavelength voxels;

calculating a second symphotic pattern of dipole values to functionally approximate the second set of subwavelength voxels; and

forming the second symphotic pattern of dipole values by modifying at least one of the plurality of control signals.

37. The method of aspect 1, wherein identifying the continuous refractive index distribution comprises determining an interferogram.

38. The method of aspect 1, wherein identifying the continuous refractive index distribution comprises measuring an interference pattern formed by an input reference wave and a target output object wave.

39. The method of aspect 1, wherein identifying the continuous refractive index distribution comprises calculating a linear solution to a multiplex volume hologram.

40. The method of aspect 1, wherein identifying the continuous refractive index distribution comprises calculating a nondispersive metamaterial media using an optimization process based on a variational principle.

41. The method of aspect 1, wherein identifying the continuous refractive index distribution comprises calculating a coupled mode modified hologram.

42. The method of aspect 1, wherein identifying the continuous refractive index distribution comprises finding a solution to an exact grating equation.

43. The method of aspect 1, wherein identifying the continuous refractive index distribution for electromagnetic embodiments comprises calculating an ideal holographic design based on a solution to a dielectric function $\epsilon(r)$ in terms of the relationship between reference field $U_R(r)$ and scattered field $U_S(r)$ such that:

$\nabla^2 U_S + \epsilon_0 \frac{\omega^2}{c^2} U_S = -(\epsilon(r) - \epsilon_0) \frac{\omega^2}{c^2} U_R$, where ω corresponds to the frequency, c corresponds to the speed of light, and wherein ϵ_0 corresponds to the permittivity of free space.

44. The method of aspect 1, wherein calculating the symphotic pattern of dipole values

comprises initially calculating a continuous polarization field $P(r)$, based on a Born approximation of the dielectric function $\epsilon(r)$, such that:

$$\nabla^2 U_S + \epsilon_0 \frac{\omega^2}{c^2} U_S = -(\epsilon(r) - \epsilon_0) \frac{\omega^2}{c^2} U_R = -\frac{\omega^2}{c^2} P(r)$$

45. The method of aspect 1, wherein modeling the continuous refractive index distribution as a plurality of subwavelength voxels comprises calculating a nondispersive metamaterial media using an optimization process based on a variational principle.

46. The method of aspect 1, wherein forming the symphotic pattern of dipole values comprises electronically tuning one or more of the dipole elements based on a parametric model optimized via a variational principle.

47. The method of aspect 46, wherein electronically tuning the one or more dipole elements comprises modifying external voltage controls of one or more dipole elements.

48. The method of aspect 1, wherein calculating the three-dimensional array of discrete dipole values comprises using machine learning to determine a functional approximation of the subwavelength voxels.

49. The method of aspect 1, wherein calculating the three-dimensional array of discrete dipole values comprises using deep learning to determine a functional approximation of the subwavelength voxels.

50. The method of aspect 1, wherein calculating the three-dimensional array of discrete dipole values comprises using convolutional neural networks to determine a functional approximation of the subwavelength voxels.

51. The method of aspect 1, wherein the three-dimensional array of discrete dipole values comprises a three-dimensional array of discrete dipole polarization states.

52. The method of aspect 51, wherein forming the symphotic pattern of dipole values comprises modifying one or more controls to select polarization states of a three-dimensional array of dipole elements.

53. The method of aspect 52, wherein the one or more controls comprises one or more voltage controls.

54. The method of aspect 1, wherein the dipole elements comprise electric I-beam LC dipole elements.

55. The method of aspect 54, wherein at least some of the electric dipole elements are tunable by adjusting one of a capacitance and an inductance.

56. The method of aspect 1, wherein the dipole elements comprise magnetic resonators for converting electromagnetic input reference waves to electromagnetic output object waves.

57. The method of aspect 56, wherein the magnetic resonators comprise at least one of split ring resonators (SRRs) and electric inductor-capacitor resonators (ELCs).

58. The method of aspect 1, wherein the dipole elements comprise dielectric resonators for conversion of optical electromagnetic input reference waves to optical electromagnetic output object waves.

59. The method of aspect 58, wherein the dielectric resonators comprise nanoparticles with fixed Mie resonances.

60. The method of aspect 58, wherein the dielectric resonators comprise nanoparticles with tunable Mie resonances.

61. The method of aspect 58, wherein the dielectric resonators comprise a set of dielectric spheres in a three-dimensional array.

62. The method of aspect 61, wherein the dielectric spheres in the three-dimensional array are set within a lower dielectric host background.

63. The method of aspect 58, wherein the dielectric resonators comprise one or more of: TiO_2, GaP, Te, PbTe, and SiC.

64. The method of aspect 58, wherein intrinsic polarizability of dielectric resonators is computed based on an effective medium theory of scattering coefficients of a single, infinitely periodic lattice of identical elements.

65. The method of aspect 1, wherein the dipole elements comprise metamaterial dielectric resonators for conversion of optical electromagnetic input reference waves to optical electromagnetic output object waves.

66. The method of aspect 65, wherein the metamaterial dielectric resonators comprise nanoparticles with fixed Mie resonances.

67. The method of aspect 65, wherein the metamaterial dielectric resonators comprise nanoparticles with tunable Mie resonances.

68. The method of aspect 65, wherein the metamaterial dielectric resonators comprise a set of metamaterial dielectric spheres in a three-dimensional array.

69. The method of aspect 68, wherein the metamaterial dielectric spheres in the three-dimensional array are set within a lower dielectric host background.

70. The method of aspect 65, wherein the metamaterial dielectric resonators comprise one or more of: TiO_2, GaP, Te, PbTe, and SiC.

71. The method of aspect 65, wherein intrinsic polarizability of the metamaterial dielectric resonators is computed based on an effective medium theory of scattering coefficients of a single, infinitely periodic lattice of identical elements.

72. The method of aspect 1, wherein the three-dimensional array of dipole elements is configured to convert M unique input reference waves to N unique output object waves, where M and N are positive integers.

73. The method of aspect 72, wherein M is equal to N.

74. The method of aspect 72, wherein M is greater than N.

75. The method of aspect 72, wherein M is smaller than N.

76. The method of aspect 1, wherein the dipole values comprise dipole moments.

77. The method of aspect 76, wherein the dipole moments are defined in terms of selectable charge magnitudes and distances between ends.

78. The method of aspect 1, wherein forming the symphotic pattern comprises a planar fabrication process of stacking layers of dipole elements.

79. The method of aspect 1, wherein forming the symphotic pattern comprises a planar fabrication process of three-dimensional printing of dipole elements.

80. The method of aspect 1, wherein forming the symphotic pattern comprises:
a planar fabrication process of three-dimensional printing of dipole elements with electric control leads, and applying voltages to the electric control leads to dynamical tune the dipole elements to attain the calculated three-dimensional dipole values.

81. The method of aspect 1, wherein forming the symphotic pattern comprises:
a planar fabrication process of stacking layers of dipole elements that have electric control leads for adjusting the dipole state of each of the dipole elements, and
applying voltages to the electric control leads to dynamical tune the dipole elements to attain the calculated three-dimensional dipole values.

82. The method of aspect 1, wherein forming the symphotic pattern comprises:
stacking of dipole elements;
depositing at least one controllable liquid crystal tuning layer; and
tuning the liquid crystal layer to dynamically tune the dipole elements to attain the calculated three-dimensional dipole values.

83. The method of aspect 1, wherein the refractive structure is dynamically reconfigurable, and wherein the three-dimensional array of dipole elements comprises an array of varactor-loaded resonators and bias lines for driving the varactors for dynamic reconfiguration of the three-dimensional array.

84. The method of aspect 1, wherein the refractive structure is dynamically reconfigurable, and wherein the three-dimensional array of dipole elements comprises an array of varactor-loaded metamaterial resonators and bias lines for driving the varactors for

dynamic reconfiguration of the three-dimensional array.

85. The method of aspect 1, wherein the symphotic structure comprises a distributed storage symphotic structure, where at least some of the plurality of input reference waves comprise read address requests and where at least some of the plurality of output object waves comprise data outputs responsive to read requests.

86. A symphotic structure, comprising:

a volumetric distribution of dipole structures with interelement spacing less than one-half of the smallest wavelength of an operational bandwidth,

wherein a dipole value of each dipole structure is selected for the volumetric distribution to convert a plurality of input reference waves to a target plurality of output object waves.

87. The symphotic structure of aspect 86, wherein the dipole value of each dipole structure is calculated using an algorithm to functionally approximate a continuous refractive index distribution calculated to convert the plurality of input reference waves to the target plurality of output object waves.

88. The symphotic structure of aspect 86 configured for use as one of: a distributed storage, an optical lens, an acoustic converter, and a three-dimensional imaging device.

89. The symphotic structure of aspect 86 configured for use as one of: a hyperspectral imaging device, encryption algorithms, machine vision, distributed learning, and chemical detection.

90. The symphotic structure of aspect 86, further comprising an imaging sensor to receive the output object waves as processed image information.

91. The symphotic structure of aspect 86, wherein the dipole structures are configured to convert electromagnetic input reference waves to electromagnetic output object waves.

92. The symphotic structure of aspect 86, wherein the dipole structures are configured to convert optical input reference waves to optical output object waves.

93. The symphotic structure of aspect 92, wherein the dipole structures are configured to convert infrared input reference waves to infrared output object waves.

94. The symphotic structure of aspect 92, wherein the dipole structures are configured to convert visible light input reference waves to visible light output object waves.

95. The symphotic structure of aspect 86 wherein at least some of the dipole structures comprise metamaterial dipole structures.

96. The symphotic structure of aspect 86, wherein the dipole structures are configured to convert radio frequency (RF) input reference waves to RF output object waves.

97. The symphotic structure of aspect 96, wherein the dipole structures are configured to

upconvert the frequency of the RF output object waves relative to the RF input reference waves.

98. The symphotic structure of aspect 96, wherein the dipole structures are configured to downconvert the frequency of the RF output object waves relative to the RF input reference waves.

99. The symphotic structure of aspect 86, wherein the dipole structures are configured to convert microwave input reference waves to microwave output object waves.

100. The symphotic structure of aspect 86, wherein the dipole structures are configured to convert terahertz input reference waves to terahertz output object waves.

101. The symphotic structure of aspect 86, wherein the dipole structures are configured to convert millimeter-wave (MMW) input reference waves to MMW output object waves.

102. The symphotic structure of aspect 86, wherein the dipole structures are configured to convert acoustic input reference waves to acoustic output object waves.

103. The symphotic structure of aspect 102, the dipole structures are configured to convert ultrasonic input reference waves to ultrasonic output object waves.

104. The symphotic structure of aspect 102, wherein the dipole structures are configured to upconvert the frequency of the acoustic output object waves relative to the acoustic input reference waves.

105. The symphotic structure of aspect 102, wherein the three-dimensional array of dipole elements is configured to downconvert the frequency of the acoustic output object waves relative to the acoustic reference waves.

106. The symphotic structure of aspect 102, wherein the dipole structures are configured to convert audible input reference waves to audible output object waves.

107. The symphotic structure of aspect 106, the dipole structures are configured to convert audible input reference waves from first and second audio channels to audible output object waves directed to different spatial locations.

108. The symphotic structure of aspect 102, wherein the dipole structures are configured to convert the acoustic input reference waves from each of a plurality of audio channels to audible output object waves that are spatially localized and fully isolated from one another.

109. The symphotic structure of aspect 87, wherein the continuous refractive index distribution comprises a continuous distribution of permittivity values.

110. The symphotic structure of aspect 87, wherein the continuous refractive index distribution comprises a continuous distribution of bulk modulus and density values.

111. The symphotic structure of aspect 86, wherein each of the plurality of input reference

waves is defined in terms of frequency, and wherein the dipole structures are configured to output a unique object wave for each unique frequency of input wave.

112. The symphotic structure of aspect 86, wherein each of the plurality of input reference waves is defined in terms of angle of incidence, and wherein each of the dipole structures are configured to output a unique object wave for each unique angle of incidence of input wave.

113. The symphotic structure of aspect 86, wherein each of the plurality of input reference waves is defined in terms of frequency and angle of incidence, and wherein the dipole structures are configured to output a unique object wave for each unique angle of incidence and frequency of input wave.

114. The symphotic structure of aspect 86, wherein each of the dipole structures have a static value to provide for a static conversion of input reference waves to output object waves.

115. The symphotic structure of aspect 86, further comprising a plurality of control signals to dynamically tune at least some of the dipole structures.

116. The symphotic structure of aspect 115, wherein each of the plurality of control signals is coupled to one of a varactor and a PIN diode, wherein each of the plurality of control signals is useable to select a polarization value of each dipole structure.

117. The symphotic structure of aspect 115, wherein at least some of the dipole elements are tunable by at least one of: electrically controllable liquid crystals, varactors, PIN diodes, MEMs, ferroelectrics, physical deformation, and mechanical actuation.

118. The symphotic structure of aspect 86, wherein at least some of the dipole structures comprise electric I-beam LC dipole elements.

119. The symphotic structure of aspect 118, wherein at least some of the dipole structures comprise are tunable by adjusting one of a capacitance and an inductance.

120. The symphotic structure of aspect 86, wherein at least some of the dipole structures comprise metamaterial electric I-beam LC dipole elements.

121. The symphotic structure of aspect 86, wherein at least some of the dipole structures comprise magnetic resonators for converting electromagnetic input reference waves to electromagnetic output object waves.

122. The symphotic structure of aspect 121, wherein the magnetic resonators comprise at least one of split ring resonators (SRRs) and electric inductor-capacitor resonators (ELCs).

123. The symphotic structure of aspect 86, wherein at least some of the dipole structures comprise metamaterial dielectric resonators for conversion of optical electromagnetic input reference waves to optical electromagnetic output object waves.

124. The symphotic structure of aspect 123, wherein the metamaterial dielectric resonators

comprise nanoparticles with fixed Mie resonances.

125. The symphotic structure of aspect 123, wherein the metamaterial dielectric resonators comprise nanoparticles with tunable Mie resonances.

126. The symphotic structure of aspect 123, wherein the metamaterial dielectric resonators comprise a set of metamaterial dielectric spheres in a three-dimensional array.

127. The symphotic structure of aspect 126, wherein the metamaterial dielectric spheres in the three-dimensional array are set within a lower dielectric host background.

128. The symphotic structure of aspect 123, wherein the metamaterial dielectric resonators comprise one or more of: TiO_2, GaP, Te, PbTe, and SiC.

129. The symphotic structure of aspect 123, wherein intrinsic polarizability of the metamaterial dielectric resonators is computed based on an effective medium theory of scattering coefficients of a single, infinitely periodic lattice of identical elements.

130. The symphotic structure of aspect 86, wherein at least some of the dipole structures comprise dielectric resonators for conversion of optical electromagnetic input reference waves to optical electromagnetic output object waves.

131. The symphotic structure of aspect 130, wherein the dielectric resonators comprise nanoparticles with fixed Mie resonances.

132. The symphotic structure of aspect 130, wherein the dielectric resonators comprise nanoparticles with tunable Mie resonances.

133. The symphotic structure of aspect 130, wherein the dielectric resonators comprise a set of dielectric spheres in a three-dimensional array.

134. The symphotic structure of aspect 133, wherein the dielectric spheres in the three-dimensional array are set within a lower dielectric host background.

135. The symphotic structure of aspect 130, wherein the dielectric resonators comprise one or more of: TiO_2, GaP, Te, PbTe, and SiC.

136. The symphotic structure of aspect 130, wherein intrinsic polarizability of the dielectric resonators is computed based on an effective medium theory of scattering coefficients of a single, infinitely periodic lattice of identical elements.

137. The symphotic structure of aspect 86, wherein the dipole structures are configured to convert M unique input reference waves to N unique output object waves, where M and N are positive integers.

138. The symphotic structure of aspect 137, wherein M is equal to N.

139. The symphotic structure of aspect 137, wherein M is greater than N.

140. The symphotic structure of aspect 137, wherein M is smaller than N.

141. The symphotic structure of aspect 86, wherein the dipole values comprise dipole moments.

142. The symphotic structure of aspect 141, wherein the dipole moments are defined in terms of selectable charge magnitudes and distances between ends.

143. The symphotic structure of aspect 86, further comprising:

an array of varactor-loaded resonators in communication with the dipole structures; and

bias lines for driving the varactors for dynamic reconfiguration of the three-dimensional array.

144. The symphotic structure of aspect 86, further comprising:

an array of varactor-loaded metamaterial resonators in communication with the metamaterial dipole structures, and

bias lines for driving the varactors for dynamic reconfiguration of the three-dimensional array.

145. A reconfigurable symphotic structure, comprising:

a volumetric distribution of dipole structures with interelement spacing less than one-half of the smallest wavelength of an operational bandwidth;

a plurality of control signals for adjusting the dipole values of the dipole structures; and

a controller for controlling the plurality of control signals to select a set of dipole values of the volumetric distribution of dipole structures to convert a plurality of input reference waves to a target plurality of output object waves.

146. The symphotic structure of aspect 145, wherein at least some of the dipole structures comprise metamaterial dipole structures.

147. The symphotic structure of aspect 145 configured for use as one of: a distributed storage, an optical lens, an acoustic converter, and a three-dimensional imaging device.

148. The symphotic structure of aspect 145 configured for use as one of: a hyperspectral imaging device, encryption algorithms, machine vision, distributed learning, chemical detection, coherence measurements, filtering, interferometry, and optical mode conversion.

149. The symphotic structure of aspect 145 configured for use as a dynamically reconfigurable optical lens.

150. The symphotic structure of aspect 145 configured for use as a dynamically reconfigurable imaging.

151. The symphotic structure of aspect 145 configured for use as a dynamically reconfigurable imaging processor.

152. The symphotic structure of aspect 145, wherein the dipole structures are configured to

filter at least one wavelength.

153. The symphotic structure of aspect 145, wherein the dipole structures are configured to convert a plurality of input reference waves from a hyperspectral wavelength range to a plurality of object output waves within a smaller wavelength range.

154. The symphotic structure of aspect 145, wherein the dipole value of each dipole structure is calculated using an algorithm to functionally approximate a continuous refractive index distribution calculated to convert the plurality of input reference waves to the target plurality of output object waves.

155. The symphotic structure of aspect 145 configured for use as one of: a distributed storage, an optical lens, an acoustic converter, and a three-dimensional imaging device.

156. The symphotic structure of aspect 145 configured for use as one of: a hyperspectral imaging device, encryption algorithms, machine vision, distributed learning, and chemical detection.

157. The symphotic structure of aspect 145, further comprising an imaging sensor to receive the output object waves as processed image information.

158. The symphotic structure of aspect 145, wherein the dipole structures are configured to convert electromagnetic input reference waves to electromagnetic output object waves.

159. The symphotic structure of aspect 145, wherein the dipole structures are configured to convert optical input reference waves to optical output object waves.

160. The symphotic structure of aspect 159, wherein the dipole structures are configured to convert infrared input reference waves to infrared output object waves.

161. The symphotic structure of aspect 159, wherein the dipole structures are configured to convert visible light input reference waves to visible light output object waves.

162. The symphotic structure of aspect 145 wherein at least some of the dipole structures comprise metamaterial dipole structures.

163. The symphotic structure of aspect 145, wherein the dipole structures are configured to convert radio frequency (RF) input reference waves to RF output object waves.

164. The symphotic structure of aspect 163, wherein the dipole structures are configured to upconvert the frequency of the RF output object waves relative to the RF input reference waves.

165. The symphotic structure of aspect 163, wherein the dipole structures are configured to downconvert the frequency of the RF output object waves relative to the RF input reference waves.

166. The symphotic structure of aspect 145, wherein the dipole structures are configured to

convert microwave input reference waves to microwave output object waves.

167. The symphotic structure of aspect 145, wherein the dipole structures are configured to convert terahertz input reference waves to terahertz output object waves.

168. The symphotic structure of aspect 145, wherein the dipole structures are configured to convert millimeter-wave (MMW) input reference waves to MMW output object waves.

169. The symphotic structure of aspect 145, wherein the dipole structures are configured to convert acoustic input reference waves to acoustic output object waves.

170. The symphotic structure of aspect 169, the dipole structures are configured to convert ultrasonic input reference waves to ultrasonic output object waves.

171. The symphotic structure of aspect 169, wherein the dipole structures are configured to upconvert the frequency of the acoustic output object waves relative to the acoustic input reference waves.

172. The symphotic structure of aspect 169, wherein the three-dimensional array of dipole elements is configured to downconvert the frequency of the acoustic output object waves relative to the acoustic reference waves.

173. The symphotic structure of aspect 169, wherein the dipole structures are configured to convert audible input reference waves to audible output object waves.

174. The symphotic structure of aspect 173, the dipole structures are configured to convert audible input reference waves from first and second audio channels to audible output object waves directed to different spatial locations.

175. The symphotic structure of aspect 173, wherein the dipole structures are configured to convert the acoustic input reference waves from each of a plurality of audio channels to audible output object waves that are spatially localized and fully isolated from one another.

176. The symphotic structure of aspect 154, wherein the continuous refractive index distribution comprises a continuous distribution of permittivity values.

177. The symphotic structure of aspect 154, wherein the continuous refractive index distribution comprises a continuous distribution of bulk modulus and density values.

178. The symphotic structure of aspect 145, wherein each of the plurality of input reference waves is defined in terms of frequency, and wherein the dipole structures are configured to output a unique object wave for each unique frequency of input wave.

179. The symphotic structure of aspect 145, wherein each of the plurality of input reference waves is defined in terms of angle of incidence, and wherein each of the dipole structures are configured to output a unique object wave for each unique angle of incidence of input wave.

180. The symphotic structure of aspect 145, wherein each of the plurality of input reference waves is defined in terms of frequency and angle of incidence, and wherein the dipole structures are configured to output a unique object wave for each unique angle of incidence and frequency of input wave.

181. The symphotic structure of aspect 145, wherein each of the dipole structures have a static value to provide for a static conversion of input reference waves to output object waves.

182. The symphotic structure of aspect 145, further comprising a plurality of control signals to dynamically tune at least some of the dipole structures.

183. The symphotic structure of aspect 182, wherein each of the plurality of control signals is coupled to one of a varactor and a PIN diode, wherein each of the plurality of control signals is useable to select a polarization value of each dipole structure.

184. The symphotic structure of aspect 182, wherein at least some of the dipole elements are tunable by at least one of: electrically controllable liquid crystals, varactors, PIN diodes, MEMs, ferroelectrics, physical deformation, and mechanical actuation.

185. The symphotic structure of aspect 145, wherein at least some of the dipole structures comprise electric I-beam LC dipole elements.

186. The symphotic structure of aspect 185, wherein at least some of the dipole structures comprise are tunable by adjusting one of a capacitance and an inductance.

187. The symphotic structure of aspect 145, wherein at least some of the dipole structures comprise metamaterial electric I-beam LC dipole elements.

188. The symphotic structure of aspect 145, wherein at least some of the dipole structures comprise magnetic resonators for converting electromagnetic input reference waves to electromagnetic output object waves.

189. The symphotic structure of aspect 188, wherein the magnetic resonators comprise at least one of split ring resonators (SRRs) and electric inductor-capacitor resonators (ELCs).

190. The symphotic structure of aspect 145, wherein at least some of the dipole structures comprise metamaterial dielectric resonators for conversion of optical electromagnetic input reference waves to optical electromagnetic output object waves.

191. The symphotic structure of aspect 190, wherein the metamaterial dielectric resonators comprise nanoparticles with fixed Mie resonances.

192. The symphotic structure of aspect 190, wherein the metamaterial dielectric resonators comprise nanoparticles with tunable Mie resonances.

193. The symphotic structure of aspect 190, wherein the metamaterial dielectric resonators comprise a set of metamaterial dielectric spheres in a three-dimensional array.

194. The symphotic structure of aspect 193, wherein the metamaterial dielectric spheres in the three-dimensional array are set within a lower dielectric host background.

195. The symphotic structure of aspect 190, wherein the metamaterial dielectric resonators comprise one or more of: TiO_2, GaP, Te, PbTe, and SiC.

196. The symphotic structure of aspect 190, wherein intrinsic polarizability of the metamaterial dielectric resonators is computed based on an effective medium theory of scattering coefficients of a single, infinitely periodic lattice of identical elements.

197. The symphotic structure of aspect 145, wherein at least some of the dipole structures comprise dielectric resonators for conversion of optical electromagnetic input reference waves to optical electromagnetic output object waves.

198. The symphotic structure of aspect 197, wherein the dielectric resonators comprise nanoparticles with fixed Mie resonances.

199. The symphotic structure of aspect 197, wherein the dielectric resonators comprise nanoparticles with tunable Mie resonances.

200. The symphotic structure of aspect 197, wherein the dielectric resonators comprise a set of dielectric spheres in a three-dimensional array.

201. The symphotic structure of aspect 200, wherein the dielectric spheres in the three-dimensional array are set within a lower dielectric host background.

202. The symphotic structure of aspect 197, wherein the dielectric resonators comprise one or more of: TiO_2, GaP, Te, PbTe, and SiC.

203. The symphotic structure of aspect 197, wherein intrinsic polarizability of the dielectric resonators is computed based on an effective medium theory of scattering coefficients of a single, infinitely periodic lattice of identical elements.

204. The symphotic structure of aspect 145, wherein the dipole structures are configured to convert M unique input reference waves to N unique output object waves, where M and N are positive integers.

205. The symphotic structure of aspect 204, wherein M is equal to N.

206. The symphotic structure of aspect 204, wherein M is greater than N.

207. The symphotic structure of aspect 204, wherein M is smaller than N.

208. The symphotic structure of aspect 145, wherein the dipole values comprise dipole moments.

209. The symphotic structure of aspect 208, wherein the dipole moments are defined in terms of selectable charge magnitudes and distances between ends.

210. The symphotic structure of aspect 145, further comprising:

an array of varactor-loaded resonators in communication with the dipole structures; and
bias lines for driving the varactors for dynamic reconfiguration of the three-dimensional array.

211. The symphotic structure of aspect 145, further comprising:
an array of varactor-loaded metamaterial resonators in communication with the metamaterial dipole structures; and
bias lines for driving the varactors for dynamic reconfiguration of the three-dimensional array.

212. A method of reconfiguring a symphotic structure, comprising:
identifying a continuous refractive index distribution to convert each of a plurality of input reference waves to a corresponding plurality of output object waves;
modeling the continuous refractive index distribution as a plurality of subwavelength voxels;
calculating a three-dimensional array of discrete dipole values (a "symphotic pattern") to functionally approximate the subwavelength voxels; and

adjusting input signals to a three-dimensional array of dipole elements to attain the symphotic pattern of dipole values for converting the plurality of input reference waves to the corresponding plurality of output object waves.

213. The method of aspect 212, wherein the three-dimensional array of dipole elements is configured to convert electromagnetic input reference waves to electromagnetic output object waves.

214. The method of aspect 213, wherein the three-dimensional array of dipole elements is configured to convert optical input reference waves to optical output object waves.

215. The method of aspect 214, wherein the three-dimensional array of dipole elements is configured to convert infrared input reference waves to infrared output object waves.

216. The method of aspect 214, wherein the three-dimensional array of dipole elements is configured to convert visible light input reference waves to visible light output object waves.

217. The method of aspect 213, wherein the dipole structures are configured to convert microwave input reference waves to microwave output object waves.

218. The method of aspect 213, wherein the dipole structures are configured to convert terahertz input reference waves to terahertz output object waves.

219. The method of aspect 213, wherein the dipole structures are configured to convert millimeter-wave (MMW) input reference waves to MMW output object waves.

220. The method of aspect 213, wherein the three-dimensional array of dipole elements is configured to convert radio frequency (RF) input reference waves to RF output object waves.

221. The method of aspect 220, wherein the three-dimensional array of dipole elements is configured to upconvert the frequency of the RF output object waves relative to the RF input reference waves.

222. The method of aspect 220, wherein the three-dimensional array of dipole elements is configured to downconvert the frequency of the RF output object waves relative to the RF input reference waves.

223. The method of aspect 220, wherein the three-dimensional array of dipole elements is configured to operate in a 77 GHz bandwidth.

224. The method of aspect 212, wherein at least some of the dipole elements comprise metamaterial dipole elements.

225. The method of aspect 212, wherein the three-dimensional array of dipole elements is configured to convert acoustic input reference waves to acoustic output object waves.

226. The method of aspect 225, wherein the three-dimensional array of dipole elements is configured to convert ultrasonic input reference waves to ultrasonic output object waves.

227. The method of aspect 225, wherein the three-dimensional array of dipole elements is configured to upconvert the frequency of the acoustic output object waves relative to the acoustic input reference waves.

228. The method of aspect 225, wherein the three-dimensional array of dipole elements is configured to downconvert the frequency of the acoustic output object waves relative to the acoustic reference waves.

229. The method of aspect 225, wherein the three-dimensional array of dipole elements is configured to convert audible input reference waves to audible output object waves.

230. The method of aspect 229, wherein the three-dimensional array of dipole elements is configured to convert audible input reference waves from first and second audio channels to audible output object waves directed to different spatial locations.

231. The method of aspect 225, wherein the three-dimensional array of dipole elements is configured to convert the acoustic input reference waves from each of a plurality of audio channels to audible output object waves that are spatially localized and fully isolated from one another.

232. The method of aspect 212, wherein the continuous refractive index distribution comprises a continuous distribution of permittivity values.

233. The method of aspect 212, wherein each subwavelength voxel is defined to have a homogenous refractive index.

234. The method of aspect 212, each of the subwavelength voxels is represented as a

polarization state.

235. The method of aspect 212, each of the subwavelength voxels is represented as a homogeneous permittivity.

236. The method of aspect 212, wherein the continuous refractive index distribution comprises a continuous distribution of bulk modulus and density values.

237. The method of aspect 212, each of the subwavelength voxels is represented as a homogeneous bulk modulus value and density value.

238. The method of aspect 212, wherein each of the plurality of input reference waves is defined in terms of frequency, and where the three-dimensional array of dipole elements is configured to output a unique object wave for each unique frequency of input wave.

239. The method of aspect 212, wherein each of the plurality of input reference waves is defined in terms of angle of incidence, such that the three-dimensional array of dipole elements to is configured to output a unique object wave for each unique angle of incidence of input wave.

240. The method of aspect 212, wherein each of the plurality of input reference waves is defined in terms of frequency and angle of incidence, such that the three-dimensional array of dipole elements to is configured to output a unique object wave for each unique angle of incidence and frequency of input wave.

241. The method of aspect 212, wherein each of the dipole elements in the three-dimensional array has a static value to provide for a static conversion of input reference waves to output object waves.

242. The method of aspect 212, wherein at least some of the dipole elements in the three-dimensional array are dynamically tunable via a plurality of control signals.

243. The method of aspect 242, further comprising:

dynamically modifying at least one of the plurality of control signals to modify the conversion of input reference waves to output object waves.

244. The method of aspect 242, wherein each of the dipole elements is coupled to one of a varactor and a PIN diode, wherein each of the plurality of control signals is useable to select a polarization value of each dipole element.

245. The method of aspect 242, wherein at least some of the dipole elements are tunable by at least one of: electrically controllable liquid crystals, varactors, PIN diodes, MEMs, ferroelectrics, physical deformation, and mechanical actuation.

246. The method of aspect 242, wherein at least some of the dipole elements are tunable

via electrical biases.

247. The method of aspect 242, further comprising:

identifying a second continuous refractive index distribution to convert each of the plurality of input reference waves to a different set of output object waves;

modeling the second continuous refractive index distribution as a second set of subwavelength voxels;

calculating a second symphotic pattern of dipole values to functionally approximate the second set of subwavelength voxels; and

forming the second symphotic pattern of dipole values by modifying at least one of the plurality of control signals.

248. The method of aspect 212, wherein identifying the continuous refractive index distribution comprises determining an interferogram.

249. The method of aspect 212, wherein identifying the continuous refractive index distribution comprises measuring an interference pattern formed by an input reference wave and a target output object wave.

250. The method of aspect 212, wherein identifying the continuous refractive index distribution comprises calculating a linear solution to a multiplex volume hologram.

251. The method of aspect 212, wherein identifying the continuous refractive index distribution comprises calculating a nondispersive metamaterial media using an optimization process based on a variational principle.

252. The method of aspect 212, wherein identifying the continuous refractive index distribution comprises calculating a coupled mode modified hologram.

253. The method of aspect 212, wherein identifying the continuous refractive index distribution comprises finding a solution to an exact grating equation.

254. The method of aspect 212, wherein identifying the continuous refractive index distribution for electromagnetic embodiments comprises calculating an ideal holographic design based on a solution to a dielectric function $\epsilon(r)$ in terms of the relationship between reference field $U_R(r)$ and scattered field $U_S(r)$ such that:

$\nabla^2 U_S + \epsilon_0 \frac{\omega^2}{c^2} U_S = -(\epsilon(r) - \epsilon_0) \frac{\omega^2}{c^2} U_R$, where ω corresponds to the frequency, c corresponds to the speed of light, and wherein ϵ_0 corresponds to the permittivity of free space.

255. The method of aspect 212, wherein calculating the symphotic pattern of dipole values

comprises initially calculating a continuous polarization field $P(r)$, based on a Born approximation of the dielectric function $\epsilon(r)$, such that:

$$\nabla^2 U_S + \epsilon_0 \frac{\omega^2}{c^2} U_S = -(\epsilon(r) - \epsilon_0) \frac{\omega^2}{c^2} U_R = -\frac{\omega^2}{c^2} P(r)$$

256. The method of aspect 212, wherein modeling the continuous refractive index distribution as a plurality of subwavelength voxels comprises calculating a nondispersive metamaterial media using an optimization process based on a variational principle.

257. The method of aspect 212, wherein forming the symphotic pattern of dipole values comprises electronically tuning one or more of the dipole elements based on a parametric model optimized via a variational principle.

258. The method of aspect 257, wherein electronically tuning the one or more dipole elements comprises modifying external voltage controls of one or more dipole elements.

259. The method of aspect 212, wherein calculating the three-dimensional array of discrete dipole values comprises using machine learning to determine a functional approximation of the subwavelength voxels.

260. The method of aspect 212, wherein calculating the three-dimensional array of discrete dipole values comprises using deep learning to determine a functional approximation of the subwavelength voxels.

261. The method of aspect 212, wherein calculating the three-dimensional array of discrete dipole values comprises using convolutional neural networks to determine a functional approximation of the subwavelength voxels.

262. The method of aspect 212, wherein the three-dimensional array of discrete dipole values comprises a three-dimensional array of discrete dipole polarization states.

263. The method of aspect 262, wherein forming the symphotic pattern of dipole values comprises modifying one or more controls to select polarization states of a three-dimensional array of dipole elements.

264. The method of aspect 263, wherein the one or more controls comprises one or more voltage controls.

265. The method of aspect 212, wherein the dipole elements comprise electric I-beam LC dipole elements.

266. The method of aspect 265, wherein at least some of the electric dipole elements are tunable by adjusting one of a capacitance and an inductance.

267. The method of aspect 212, wherein the dipole elements comprise magnetic resonators for converting electromagnetic input reference waves to electromagnetic output object waves.

268. The method of aspect 267, wherein the magnetic resonators comprise at least one of split ring resonators (SRRs) and electric inductor-capacitor resonators (ELCs).

269. The method of aspect 212, wherein the dipole elements comprise dielectric resonators for conversion of optical electromagnetic input reference waves to optical electromagnetic output object waves.

270. The method of aspect 269, wherein the dielectric resonators comprise nanoparticles with fixed Mie resonances.

271. The method of aspect 269, wherein the dielectric resonators comprise nanoparticles with tunable Mie resonances.

272. The method of aspect 269, wherein the dielectric resonators comprise a set of dielectric spheres in a three-dimensional array.

273. The method of aspect 272, wherein the dielectric spheres in the three-dimensional array are set within a lower dielectric host background.

274. The method of aspect 269, wherein the dielectric resonators comprise one or more of: TiO_2, GaP, Te, PbTe, and SiC.

275. The method of aspect 269, wherein intrinsic polarizability of dielectric resonators is computed based on an effective medium theory of scattering coefficients of a single, infinitely periodic lattice of identical elements.

276. The method of aspect 212, wherein the dipole elements comprise metamaterial dielectric resonators for conversion of optical electromagnetic input reference waves to optical electromagnetic output object waves.

277. The method of aspect 276, wherein the metamaterial dielectric resonators comprise nanoparticles with fixed Mie resonances.

278. The method of aspect 276, wherein the metamaterial dielectric resonators comprise nanoparticles with tunable Mie resonances.

279. The method of aspect 276, wherein the metamaterial dielectric resonators comprise a set of metamaterial dielectric spheres in a three-dimensional array.

280. The method of aspect 279, wherein the metamaterial dielectric spheres in the three-dimensional array are set within a lower dielectric host background.

281. The method of aspect 276, wherein the metamaterial dielectric resonators comprise one or more of: TiO_2, GaP, Te, PbTe, and SiC.

282. The method of aspect 276, wherein intrinsic polarizability of the metamaterial dielectric resonators is computed based on an effective medium theory of scattering coefficients of a single, infinitely periodic lattice of identical elements.

283. The method of aspect 212, wherein the three-dimensional array of dipole elements is configured to convert M unique input reference waves to N unique output object waves, where M and N are positive integers.

284. The method of aspect 283, wherein M is equal to N.

285. The method of aspect 283, wherein M is greater than N.

286. The method of aspect 283, wherein M is smaller than N.

287. The method of aspect 212, wherein the dipole values comprise dipole moments.

288. The method of aspect 287, wherein the dipole moments are defined in terms of selectable charge magnitudes and distances between ends.

289. The method of aspect 212, wherein forming the symphotic pattern comprises a planar fabrication process of stacking layers of dipole elements.

290. The method of aspect 212, wherein forming the symphotic pattern comprises a planar fabrication process of three-dimensional printing of dipole elements.

291. The method of aspect 212, wherein forming the symphotic pattern comprises:

a planar fabrication process of three-dimensional printing of dipole elements with electric control leads, and

applying voltages to the electric control leads to dynamical tune the dipole elements to attain the calculated three-dimensional dipole values.

292. The method of aspect 212, wherein forming the symphotic pattern comprises:

a planar fabrication process of stacking layers of dipole elements that have electric control leads for adjusting the dipole state of each of the dipole elements, and

applying voltages to the electric control leads to dynamical tune the dipole elements to attain the calculated three-dimensional dipole values.

293. The method of aspect 212, wherein forming the symphotic pattern comprises:

stacking of dipole elements;

depositing at least one controllable liquid crystal tuning layer; and

tuning the liquid crystal layer to dynamically tune the dipole elements to attain the calculated three-dimensional dipole values.

294. The method of aspect 212, wherein the refractive structure is dynamically reconfigurable, and wherein the three-dimensional array of dipole elements comprises an array of varactor-loaded resonators and bias lines for driving the varactors for dynamic reconfiguration of the three-dimensional array.

295. The method of aspect 212, wherein the refractive structure is dynamically reconfigurable, and wherein the three-dimensional array of dipole elements comprises an

array of varactor-loaded metamaterial resonators and bias lines for driving the varactors for dynamic reconfiguration of the three-dimensional array.

296. The method of aspect 212, wherein the symphotic structure comprises a distributed storage symphotic structure, where at least some of the plurality of input reference waves comprise read address requests and where at least some of the plurality of output object waves comprise data outputs responsive to read requests.

297. A method of forming a symphotic structure, comprising:

retrieving a symphotic pattern from an electronic datastore, wherein the symphotic pattern defines a three-dimensional array of discrete dipole values that are calculated to collectively operate to convert each of a plurality of input reference waves to a corresponding plurality of output object waves; and

adjusting a dipole value of each of a plurality of dipole elements within a three-dimensional array of dipole elements based on the retrieved symphotic pattern.

298. A method of aspect 297, wherein adjusting the dipole values based on the retrieved symphotic pattern comprises matching the dipole values of the three-dimensional array of dipole elements with the symphotic pattern exactly.

299. A method of aspect 297, wherein adjusting the dipole values based on the retrieved symphotic pattern comprises adjusting the dipole values of the three-dimensional array of dipole elements to approximate the symphotic pattern within the tunability limitations of the three-dimensional array of dipole elements.

300. A method of aspect 297, wherein adjusting a dipole value of each of a plurality of dipole elements comprises adjusting a voltage control.

301. A method of aspect 297, wherein adjusting a dipole value of each of a plurality of dipole elements comprises adjusting dipole values of multiple dipole elements as a group.

302. The method of aspect 297, wherein the three-dimensional array of dipole elements is configured to convert electromagnetic input reference waves to electromagnetic output object waves.

303. The method of aspect 302, wherein the three-dimensional array of dipole elements is configured to convert optical input reference waves to optical output object waves.

304. The method of aspect 303, wherein the three-dimensional array of dipole elements is configured to convert infrared input reference waves to infrared output object waves.

305. The method of aspect 303, wherein the three-dimensional array of dipole elements is configured to convert visible light input reference waves to visible light output object waves.

306. The method of aspect 302, wherein the dipole structures are configured to convert

microwave input reference waves to microwave output object waves.

307. The method of aspect 302, wherein the dipole structures are configured to convert terahertz input reference waves to terahertz output object waves.

308. The method of aspect 302, wherein the dipole structures are configured to convert millimeter-wave (MMW) input reference waves to MMW output object waves.

309. The method of aspect 302, wherein the three-dimensional array of dipole elements is configured to convert radio frequency (RF) input reference waves to RF output object waves.

310. The method of aspect 309, wherein the three-dimensional array of dipole elements is configured to upconvert the frequency of the RF output object waves relative to the RF input reference waves.

311. The method of aspect 309, wherein the three-dimensional array of dipole elements is configured to downconvert the frequency of the RF output object waves relative to the RF input reference waves.

312. The method of aspect 309, wherein the three-dimensional array of dipole elements is configured to operate in a 77 GHz bandwidth.

313. The method of aspect 297, wherein at least some of the dipole elements comprise metamaterial dipole elements.

314. The method of aspect 297, wherein the three-dimensional array of dipole elements is configured to convert acoustic input reference waves to acoustic output object waves.

315. The method of aspect 314, wherein the three-dimensional array of dipole elements is configured to convert ultrasonic input reference waves to ultrasonic output object waves.

316. The method of aspect 314, wherein the three-dimensional array of dipole elements is configured to upconvert the frequency of the acoustic output object waves relative to the acoustic input reference waves.

317. The method of aspect 314, wherein the three-dimensional array of dipole elements is configured to downconvert the frequency of the acoustic output object waves relative to the acoustic reference waves.

318. The method of aspect 314, wherein the three-dimensional array of dipole elements is configured to convert audible input reference waves to audible output object waves.

319. The method of aspect 318, wherein the three-dimensional array of dipole elements is configured to convert audible input reference waves from first and second audio channels to audible output object waves directed to different spatial locations.

320. The method of aspect 314, wherein the three-dimensional array of dipole elements is configured to convert the acoustic input reference waves from each of a plurality of audio

channels to audible output object waves that are spatially localized and fully isolated from one another.

321. The method of aspect 297, wherein the continuous refractive index distribution comprises a continuous distribution of permittivity values.

322. The method of aspect 297, wherein each subwavelength voxel is defined to have a homogenous refractive index.

323. The method of aspect 297, each of the subwavelength voxels is represented as a polarization state.

324. The method of aspect 297, each of the subwavelength voxels is represented as a homogeneous permittivity.

325. The method of aspect 297, wherein the continuous refractive index distribution comprises a continuous distribution of bulk modulus and density values.

326. The method of aspect 297, each of the subwavelength voxels is represented as a homogeneous bulk modulus value and density value.

327. The method of aspect 297, wherein each of the plurality of input reference waves is defined in terms of frequency, and where the three-dimensional array of dipole elements is configured to output a unique object wave for each unique frequency of input wave.

328. The method of aspect 297, wherein each of the plurality of input reference waves is defined in terms of angle of incidence, such that the three-dimensional array of dipole elements to is configured to output a unique object wave for each unique angle of incidence of input wave.

329. The method of aspect 297, wherein each of the plurality of input reference waves is defined in terms of frequency and angle of incidence, such that the three-dimensional array of dipole elements to is configured to output a unique object wave for each unique angle of incidence and frequency of input wave.

330. The method of aspect 297, wherein each of the dipole elements in the three-dimensional array has a static value to provide for a static conversion of input reference waves to output object waves.

331. The method of aspect 297, wherein at least some of the dipole elements in the three-dimensional array are dynamically tunable via a plurality of control signals.

332. The method of aspect 331, further comprising:

dynamically modifying at least one of the plurality of control signals to modify the conversion of input reference waves to output object waves.

333. The method of aspect 331, wherein each of the dipole elements is coupled to one of a

varactor and a PIN diode, wherein each of the plurality of control signals is useable to select a polarization value of each dipole element.

334. The method of aspect 331, wherein at least some of the dipole elements are tunable by at least one of: electrically controllable liquid crystals, varactors, PIN diodes, MEMs, ferroelectrics, physical deformation, and mechanical actuation.

335. The method of aspect 331, wherein at least some of the dipole elements are tunable via electrical biases.

336. The method of aspect 331, further comprising:

identifying a second continuous refractive index distribution to convert each of the plurality of input reference waves to a different set of output object waves;

modeling the second continuous refractive index distribution as a second set of subwavelength voxels;

calculating a second symphotic pattern of dipole values to functionally approximate the second set of subwavelength voxels; and

forming the second symphotic pattern of dipole values by modifying at least one of the plurality of control signals.

337. The method of aspect 297, wherein identifying the continuous refractive index distribution comprises determining an interferogram.

338. The method of aspect 297, wherein identifying the continuous refractive index distribution comprises measuring an interference pattern formed by an input reference wave and a target output object wave.

339. The method of aspect 297, wherein identifying the continuous refractive index distribution comprises calculating a linear solution to a multiplex volume hologram.

340. The method of aspect 297, wherein identifying the continuous refractive index distribution comprises calculating a nondispersive metamaterial media using an optimization process based on a variational principle.

341. The method of aspect 297, wherein identifying the continuous refractive index distribution comprises calculating a coupled mode modified hologram.

342. The method of aspect 297, wherein identifying the continuous refractive index distribution comprises finding a solution to an exact grating equation.

343. The method of aspect 297, wherein identifying the continuous refractive index distribution for electromagnetic embodiments comprises calculating an ideal holographic design based on a solution to a dielectric function $\epsilon(r)$ in terms of the relationship between reference field $U_R(r)$ and scattered field $U_S(r)$ such that:

$\nabla^2 U_S + \epsilon_0 \frac{\omega^2}{c^2} U_S = -(\epsilon(r) - \epsilon_0) \frac{\omega^2}{c^2} U_R$, where ω corresponds to the frequency, c corresponds to the speed of light, and wherein ϵ_0 corresponds to the permittivity of free space.

344. The method of aspect 297, wherein calculating the symphotic pattern of dipole values comprises initially calculating a continuous polarization field $P(r)$, based on a Born approximation of the dielectric function $\epsilon(r)$, such that:

$$\nabla^2 U_S + \epsilon_0 \frac{\omega^2}{c^2} U_S = -(\epsilon(r) - \epsilon_0) \frac{\omega^2}{c^2} U_R = -\frac{\omega^2}{c^2} P(r)$$

345. The method of aspect 297, wherein modeling the continuous refractive index distribution as a plurality of subwavelength voxels comprises calculating a nondispersive metamaterial media using an optimization process based on a variational principle.

346. The method of aspect 297, wherein forming the symphotic pattern of dipole values comprises electronically tuning one or more of the dipole elements based on a parametric model optimized via a variational principle.

347. The method of aspect 346, wherein electronically tuning the one or more dipole elements comprises modifying external voltage controls of one or more dipole elements.

348. The method of aspect 297, wherein calculating the three-dimensional array of discrete dipole values comprises using machine learning to determine a functional approximation of the subwavelength voxels.

349. The method of aspect 297, wherein calculating the three-dimensional array of discrete dipole values comprises using deep learning to determine a functional approximation of the subwavelength voxels.

350. The method of aspect 297, wherein calculating the three-dimensional array of discrete dipole values comprises using convolutional neural networks to determine a functional approximation of the subwavelength voxels.

351. The method of aspect 297, wherein the three-dimensional array of discrete dipole values comprises a three-dimensional array of discrete dipole polarization states.

352. The method of aspect 351, wherein forming the symphotic pattern of dipole values comprises modifying one or more controls to select polarization states of a three-dimensional array of dipole elements.

353. The method of aspect 352, wherein the one or more controls comprises one or more voltage controls.

354. The method of aspect 297, wherein the dipole elements comprise electric I-beam LC dipole elements.

355. The method of aspect 354, wherein at least some of the electric dipole elements are tunable by adjusting one of a capacitance and an inductance.

356. The method of aspect 297, wherein the dipole elements comprise magnetic resonators for converting electromagnetic input reference waves to electromagnetic output object waves.

357. The method of aspect 356, wherein the magnetic resonators comprise at least one of split ring resonators (SRRs) and electric inductor-capacitor resonators (ELCs).

358. The method of aspect 297, wherein the dipole elements comprise dielectric resonators for conversion of optical electromagnetic input reference waves to optical electromagnetic output object waves.

359. The method of aspect 358, wherein the dielectric resonators comprise nanoparticles with fixed Mie resonances.

360. The method of aspect 358, wherein the dielectric resonators comprise nanoparticles with tunable Mie resonances.

361. The method of aspect 358, wherein the dielectric resonators comprise a set of dielectric spheres in a three-dimensional array.

362. The method of aspect 361, wherein the dielectric spheres in the three-dimensional array are set within a lower dielectric host background.

363. The method of aspect 358, wherein the dielectric resonators comprise one or more of: TiO_2, GaP, Te, PbTe, and SiC.

364. The method of aspect 358, wherein intrinsic polarizability of dielectric resonators is computed based on an effective medium theory of scattering coefficients of a single, infinitely periodic lattice of identical elements.

365. The method of aspect 297, wherein the dipole elements comprise metamaterial dielectric resonators for conversion of optical electromagnetic input reference waves to optical electromagnetic output object waves.

366. The method of aspect 365, wherein the metamaterial dielectric resonators comprise nanoparticles with fixed Mie resonances.

367. The method of aspect 365, wherein the metamaterial dielectric resonators comprise nanoparticles with tunable Mie resonances.

368. The method of aspect 365, wherein the metamaterial dielectric resonators comprise a set of metamaterial dielectric spheres in a three-dimensional array.

369. The method of aspect 368, wherein the metamaterial dielectric spheres in the three-dimensional array are set within a lower dielectric host background.

370. The method of aspect 365, wherein the metamaterial dielectric resonators comprise

one or more of: TiO_2, GaP, Te, PbTe, and SiC.

371. The method of aspect 365, wherein intrinsic polarizability of the metamaterial dielectric resonators is computed based on an effective medium theory of scattering coefficients of a single, infinitely periodic lattice of identical elements.

372. The method of aspect 297, wherein the three-dimensional array of dipole elements is configured to convert M unique input reference waves to N unique output object waves, where M and N are positive integers.

373. The method of aspect 372, wherein M is equal to N.

374. The method of aspect 372, wherein M is greater than N.

375. The method of aspect 372, wherein M is smaller than N.

376. The method of aspect 297, wherein the dipole values comprise dipole moments.

377. The method of aspect 376, wherein the dipole moments are defined in terms of selectable charge magnitudes and distances between ends.

378. The method of aspect 297, wherein forming the symphotic pattern comprises a planar fabrication process of stacking layers of dipole elements.

379. The method of aspect 297, wherein forming the symphotic pattern comprises a planar fabrication process of three-dimensional printing of dipole elements.

380. The method of aspect 297, wherein forming the symphotic pattern comprises:

a planar fabrication process of three-dimensional printing of dipole elements with electric control leads, and

applying voltages to the electric control leads to dynamical tune the dipole elements to attain the calculated three-dimensional dipole values.

381. The method of aspect 297, wherein forming the symphotic pattern comprises:

a planar fabrication process of stacking layers of dipole elements that have electric control leads for adjusting the dipole state of each of the dipole elements, and

applying voltages to the electric control leads to dynamical tune the dipole elements to attain the calculated three-dimensional dipole values.

382. The method of aspect 297, wherein forming the symphotic pattern comprises:

stacking of dipole elements;

depositing at least one controllable liquid crystal tuning layer; and

tuning the liquid crystal layer to dynamically tune the dipole elements to attain the calculated three-dimensional dipole values.

383. The method of aspect 297, wherein the refractive structure is dynamically reconfigurable, and wherein the three-dimensional array of dipole elements comprises an

array of varactor-loaded resonators and bias lines for driving the varactors for dynamic reconfiguration of the three-dimensional array.

384. The method of aspect 297, wherein the refractive structure is dynamically reconfigurable, and wherein the three-dimensional array of dipole elements comprises an array of varactor-loaded metamaterial resonators and bias lines for driving the varactors for dynamic reconfiguration of the three-dimensional array.

385. The method of aspect 297, wherein the symphotic structure comprises a distributed storage symphotic structure, where at least some of the plurality of input reference waves comprise read address requests and where at least some of the plurality of output object waves comprise data outputs responsive to read requests.

386. A dynamically reconfigurable symphotic structure, comprising:

a volumetric distribution of discrete dipole elements in a three-dimensional array with subwavelength interelement spacings;

a plurality of dipole controls for selectively modifying dipole values of at least some of the dipole elements in the three-dimensional array of dipole elements;

a storage medium storing a plurality of symphotic patterns,

wherein each of the plurality of symphotic patterns corresponds to a unique mapping of input reference waves to output object waves, and

wherein each of the plurality of symphotic patterns defines a unique three-dimensional array of discrete dipole values; and

control circuitry to read a symphotic pattern in the storage medium and cause the dipole controls to modify one or more dipole values of one or more dipole elements based on the read symphotic pattern.

387. The structure of aspect 386, wherein the dipole value of each dipole structure is calculated using an algorithm to functionally approximate a continuous refractive index distribution calculated to convert the plurality of input reference waves to the target plurality of output object waves.

388. The structure of aspect 386 configured for use as one of: a distributed storage, an optical lens, an acoustic converter, and a three-dimensional imaging device.

389. The structure of aspect 386 configured for use as one of: a hyperspectral imaging device, encryption algorithms, machine vision, distributed learning, and chemical detection.

390. The structure of aspect 386, further comprising an imaging sensor to receive the output object waves as processed image information.

391. The structure of aspect 386, wherein the dipole structures are configured to convert

electromagnetic input reference waves to electromagnetic output object waves.

392. The structure of aspect 386, wherein the dipole structures are configured to convert optical input reference waves to optical output object waves.

393. The structure of aspect 392, wherein the dipole structures are configured to convert infrared input reference waves to infrared output object waves.

394. The structure of aspect 392, wherein the dipole structures are configured to convert visible light input reference waves to visible light output object waves.

395. The structure of aspect 386 wherein at least some of the dipole structures comprise metamaterial dipole structures.

396. The structure of aspect 386, wherein the dipole structures are configured to convert radio frequency (RF) input reference waves to RF output object waves.

397. The structure of aspect 396, wherein the dipole structures are configured to upconvert the frequency of the RF output object waves relative to the RF input reference waves.

398. The structure of aspect 396, wherein the dipole structures are configured to downconvert the frequency of the RF output object waves relative to the RF input reference waves.

399. The structure of aspect 386, wherein the dipole structures are configured to convert microwave input reference waves to microwave output object waves.

400. The structure of aspect 386, wherein the dipole structures are configured to convert terahertz input reference waves to terahertz output object waves.

401. The structure of aspect 386, wherein the dipole structures are configured to convert millimeter-wave (MMW) input reference waves to MMW output object waves.

402. The structure of aspect 386, wherein the dipole structures are configured to convert acoustic input reference waves to acoustic output object waves.

403. The structure of aspect 402, the dipole structures are configured to convert ultrasonic input reference waves to ultrasonic output object waves.

404. The structure of aspect 402, wherein the dipole structures are configured to upconvert the frequency of the acoustic output object waves relative to the acoustic input reference waves.

405. The structure of aspect 402, wherein the three-dimensional array of dipole elements is configured to downconvert the frequency of the acoustic output object waves relative to the acoustic reference waves.

406. The structure of aspect 402, wherein the dipole structures are configured to convert audible input reference waves to audible output object waves.

407. The structure of aspect 406, the dipole structures are configured to convert audible input reference waves from first and second audio channels to audible output object waves directed to different spatial locations.

408. The structure of aspect 402, wherein the dipole structures are configured to convert the acoustic input reference waves from each of a plurality of audio channels to audible output object waves that are spatially localized and fully isolated from one another.

409. The structure of aspect 387, wherein the continuous refractive index distribution comprises a continuous distribution of permittivity values.

410. The structure of aspect 387, wherein the continuous refractive index distribution comprises a continuous distribution of bulk modulus and density values.

411. The structure of aspect 386, wherein each of the plurality of input reference waves is defined in terms of frequency, and wherein the dipole structures are configured to output a unique object wave for each unique frequency of input wave.

412. The structure of aspect 386, wherein each of the plurality of input reference waves is defined in terms of angle of incidence, and wherein each of the dipole structures are configured to output a unique object wave for each unique angle of incidence of input wave.

413. The structure of aspect 386, wherein each of the plurality of input reference waves is defined in terms of frequency and angle of incidence, and wherein the dipole structures are configured to output a unique object wave for each unique angle of incidence and frequency of input wave.

414. The structure of aspect 386, wherein each of the dipole structures have a static value to provide for a static conversion of input reference waves to output object waves.

415. The structure of aspect 386, further comprising a plurality of control signals to dynamically tune at least some of the dipole structures.

416. The structure of aspect 415, wherein each of the plurality of control signals is coupled to one of a varactor and a PIN diode, wherein each of the plurality of control signals is useable to select a polarization value of each dipole structure.

417. The structure of aspect 415, wherein at least some of the dipole elements are tunable by at least one of: electrically controllable liquid crystals, varactors, PIN diodes, MEMs, ferroelectrics, physical deformation, and mechanical actuation.

418. The structure of aspect 386, wherein at least some of the dipole structures comprise electric I-beam LC dipole elements.

419. The structure of aspect 418, wherein at least some of the dipole structures comprise are tunable by adjusting one of a capacitance and an inductance.

420. The structure of aspect 386, wherein at least some of the dipole structures comprise metamaterial electric I-beam LC dipole elements.

421. The structure of aspect 386, wherein at least some of the dipole structures comprise magnetic resonators for converting electromagnetic input reference waves to electromagnetic output object waves.

422. The structure of aspect 421, wherein the magnetic resonators comprise at least one of split ring resonators (SRRs) and electric inductor-capacitor resonators (ELCs).

423. The structure of aspect 386, wherein at least some of the dipole structures comprise metamaterial dielectric resonators for conversion of optical electromagnetic input reference waves to optical electromagnetic output object waves.

424. The structure of aspect 423, wherein the metamaterial dielectric resonators comprise nanoparticles with fixed Mie resonances.

425. The structure of aspect 423, wherein the metamaterial dielectric resonators comprise nanoparticles with tunable Mie resonances.

426. The structure of aspect 423, wherein the metamaterial dielectric resonators comprise a set of metamaterial dielectric spheres in a three-dimensional array.

427. The structure of aspect 426, wherein the metamaterial dielectric spheres in the three-dimensional array are set within a lower dielectric host background.

428. The structure of aspect 423, wherein the metamaterial dielectric resonators comprise one or more of: TiO_2, GaP, Te, PbTe, and SiC.

429. The structure of aspect 423, wherein intrinsic polarizability of the metamaterial dielectric resonators is computed based on an effective medium theory of scattering coefficients of a single, infinitely periodic lattice of identical elements.

430. The structure of aspect 386, wherein at least some of the dipole structures comprise dielectric resonators for conversion of optical electromagnetic input reference waves to optical electromagnetic output object waves.

431. The structure of aspect 430, wherein the dielectric resonators comprise nanoparticles with fixed Mie resonances.

432. The structure of aspect 430, wherein the dielectric resonators comprise nanoparticles with tunable Mie resonances.

433. The structure of aspect 430, wherein the dielectric resonators comprise a set of dielectric spheres in a three-dimensional array.

434. The structure of aspect 433, wherein the dielectric spheres in the three-dimensional array are set within a lower dielectric host background.

435. The structure of aspect 430, wherein the dielectric resonators comprise one or more of: TiO_2, GaP, Te, PbTe, and SiC.

436. The structure of aspect 430, wherein intrinsic polarizability of the dielectric resonators is computed based on an effective medium theory of scattering coefficients of a single, infinitely periodic lattice of identical elements.

437. The structure of aspect 386, wherein the dipole structures are configured to convert M unique input reference waves to N unique output object waves, where M and N are positive integers.

438. The structure of aspect 437, wherein M is equal to N.

439. The structure of aspect 437, wherein M is greater than N.

440. The structure of aspect 437, wherein M is smaller than N.

441. The structure of aspect 386, wherein the dipole values comprise dipole moments.

442. The structure of aspect 441, wherein the dipole moments are defined in terms of selectable charge magnitudes and distances between ends.

443. The structure of aspect 386, further comprising:

an array of varactor-loaded resonators in communication with the dipole structures; and

bias lines for driving the varactors for dynamic reconfiguration of the three-dimensional array.

444. The structure of aspect 386, further comprising:

an array of varactor-loaded metamaterial resonators in communication with the metamaterial dipole structures; and

bias lines for driving the varactors for dynamic reconfiguration of the three-dimensional array.

[00108] Many existing computing devices and infrastructures may be used in combination with the presently described systems and methods. Some of the infrastructure that can be used with embodiments disclosed herein is already available, such as general-purpose computers, computer programming tools and techniques, digital storage media, and communication links. A computing device or controller may include a processor, such as a microprocessor, a microcontroller, logic circuitry, or the like. A processor may include one or more special-purpose processing devices, such as application-specific integrated circuits (ASICs), programmable array logic (PAL), programmable logic array (PLA), programmable logic device (PLD), field-programmable gate array (FPGA), or other customizable and/or programmable device. The computing device may also include a machine-readable storage device, such as non-volatile memory, static RAM, dynamic RAM, ROM, CD-ROM, disk, tape,

magnetic, optical, flash memory, or another machine-readable storage medium. Various aspects of certain embodiments may be implemented using hardware, software, firmware, or a combination thereof.

[00109] The components of the disclosed embodiments, as generally described and illustrated in the figures herein, could be arranged and designed in a wide variety of different configurations. Furthermore, the features, structures, and operations associated with one embodiment may be applied to or combined with the features, structures, or operations described in conjunction with another embodiment. In many instances, well-known structures, materials, or operations are not shown or described in detail in order to avoid obscuring aspects of this disclosure.

[00110] The embodiments of the systems and methods provided within this disclosure are not intended to limit the scope of the disclosure but are merely representative of possible embodiments. In addition, the steps of a method do not necessarily need to be executed in any specific order, or even sequentially, nor do the steps need to be executed only once.

[00111] This disclosure has been made with reference to various exemplary embodiments, including the best mode. However, those skilled in the art will recognize that changes and modifications may be made to the exemplary embodiments without departing from the scope of the present disclosure. While the principles of this disclosure have been shown in various embodiments, many modifications of structure, arrangements, proportions, elements, materials, and components may be adapted for a specific environment and/or operating requirements without departing from the principles and scope of this disclosure. These and other changes or modifications are intended to be included within the scope of the present disclosure.

[00112] This disclosure is to be regarded in an illustrative rather than a restrictive sense, and all such modifications are intended to be included within the scope thereof. Likewise, benefits, other advantages, and solutions to problems have been described above with regard to various embodiments. However, benefits, advantages, solutions to problems, and any element(s) that may cause any benefit, advantage, or solution to occur or become more pronounced are not to be construed as a critical, required, or essential feature or element. This disclosure should, therefore, be determined to encompass at least the following claims.

What is claimed is:

1. A method of forming a symphotic structure, comprising:

identifying a continuous refractive index distribution to convert each of a plurality of input reference waves to a corresponding plurality of output object waves;

modeling the continuous refractive index distribution as a plurality of subwavelength voxels;

calculating a three-dimensional array of discrete dipole values (a "symphotic pattern") to functionally approximate the subwavelength voxels; and

forming the symphotic pattern of dipole values as a three-dimensional array of dipole elements to convert the plurality of input reference waves to the corresponding plurality of output object waves.

2. The method of claim 1, wherein the three-dimensional array of dipole elements is configured to convert electromagnetic input reference waves to electromagnetic output object waves.

3. The method of any of claims 1-2, wherein at least some of the dipole elements comprise metamaterial dipole elements.

4. The method of claim 1, wherein the three-dimensional array of dipole elements is configured to convert acoustic input reference waves to acoustic output object waves.

5. The method of claim 4, wherein the three-dimensional array of dipole elements is configured to convert the acoustic input reference waves from each of a plurality of audio channels to audible output object waves that are spatially localized and fully isolated from one another.

6. The method of any of claims 1-3, wherein at least some of the dipole elements in the three-dimensional array are dynamically tunable via a plurality of control signals.

7. The method of claim 6, further comprising:

dynamically modifying at least one of the plurality of control signals to modify the conversion of input reference waves to output object waves.

8. The method of claim 6, wherein each of the dipole elements is coupled to one of a varactor and a PIN diode, wherein each of the plurality of control signals is useable to select a polarization value of each dipole element.

9. The method of claim 6, wherein at least some of the dipole elements are tunable by at least one of: electrically controllable liquid crystals, varactors, PIN diodes, MEMs, ferroelectrics, physical deformation, and mechanical actuation.

10. The method of claim 6, wherein at least some of the dipole elements are tunable via electrical biases.

11. The method of claim 6, further comprising:

identifying a second continuous refractive index distribution to convert each of the plurality of input reference waves to a different set of output object waves;

modeling the second continuous refractive index distribution as a second set of subwavelength voxels;

calculating a second symphotic pattern of dipole values to functionally approximate the second set of subwavelength voxels; and

forming the second symphotic pattern of dipole values by modifying at least one of the plurality of control signals.

12. The method of any of claims 1-6, wherein forming the symphotic pattern of dipole values comprises electronically tuning one or more of the dipole elements based on a parametric model optimized via a variational principle.

13. The method of any of claims 1-3, wherein the dipole elements comprise dielectric resonators for conversion of optical electromagnetic input reference waves to optical electromagnetic output object waves.

14. The method of any of claims 1, wherein the dipole elements comprise metamaterial dielectric resonators for conversion of optical electromagnetic input reference waves to optical electromagnetic output object waves.

15. The method of any of claims 1-3, wherein the refractive structure is dynamically reconfigurable, and wherein the three-dimensional array of dipole elements comprises an array of varactor-loaded metamaterial resonators and bias lines for driving the varactors for dynamic reconfiguration of the three-dimensional array.

16. A symphotic structure, comprising:

a volumetric distribution of dipole structures with interelement spacing less than one-half of the smallest wavelength of an operational bandwidth,

wherein a dipole value of each dipole structure is selected for the volumetric distribution to convert a plurality of input reference waves to a target plurality of output object waves.

17. The symphotic structure of claim 16, wherein each of the plurality of input reference waves is defined in terms of frequency and angle of incidence, and wherein the dipole structures are configured to output a unique object wave for each unique angle of incidence and frequency of input wave.

18. The symphotic structure of claims 16 or 17, further comprising:

an array of varactor-loaded metamaterial resonators in communication with the metamaterial dipole structures, and

bias lines for driving the varactors for dynamic reconfiguration of the three-dimensional array.

19. A reconfigurable symphotic structure, comprising:

a volumetric distribution of dipole structures with interelement spacing less than one-half of the smallest wavelength of an operational bandwidth;

a plurality of control signals for adjusting the dipole values of the dipole structures; and

a controller for controlling the plurality of control signals to select a set of dipole values of the volumetric distribution of dipole structures to convert a plurality of input reference waves to a target plurality of output object waves.

20. The symphotic structure of claim 19, wherein at least some of the dipole structures comprise metamaterial dipole structures.

21. The symphotic structure of claim 19 or 20 configured for use as a dynamically reconfigurable imaging processor.

22. The symphotic structure of any of claims 19-21, wherein the dipole structures are configured to filter at least one wavelength.

23. The symphotic structure of any of claims 19-21, wherein the dipole structures are configured to convert a plurality of input reference waves from a hyperspectral wavelength range to a plurality of object output waves within a smaller wavelength range.

24. The symphotic structure of any of claims 19-23 wherein at least some of the dipole structures comprise metamaterial dipole structures.

25. The symphotic structure of claim 19 or 20 wherein the dipole structures are configured to convert radio frequency (RF) input reference waves to RF output object waves.

26. The symphotic structure of claim 25, wherein the dipole structures are configured to upconvert the frequency of the RF output object waves relative to the RF input reference waves.

27. The symphotic structure of any of claims 19-23, wherein at least some of the dipole structures comprise metamaterial dielectric resonators for conversion of optical electromagnetic input reference waves to optical electromagnetic output object waves.

28. The symphotic structure of claim 27, wherein the metamaterial dielectric resonators comprise a set of metamaterial dielectric spheres in a three-dimensional array.

29. A method of reconfiguring a symphotic structure, comprising:

identifying a continuous refractive index distribution to convert each of a plurality of input reference waves to a corresponding plurality of output object waves;

modeling the continuous refractive index distribution as a plurality of subwavelength voxels;

calculating a three-dimensional array of discrete dipole values (a "symphotic pattern") to functionally approximate the subwavelength voxels; and

adjusting input signals to a three-dimensional array of dipole elements to attain the symphotic pattern of dipole values for converting the plurality of input reference waves to the corresponding plurality of output object waves.

30. A dynamically reconfigurable symphotic structure, comprising:

a volumetric distribution of discrete dipole elements in a three-dimensional array with subwavelength interelement spacings;

a plurality of dipole controls for selectively modifying dipole values of at least some of the dipole elements in the three-dimensional array of dipole elements;

a storage medium storing a plurality of symphotic patterns,

wherein each of the plurality of symphotic patterns corresponds to a unique mapping of input reference waves to output object waves, and

wherein each of the plurality of symphotic patterns defines a unique three-dimensional array of discrete dipole values; and

control circuitry to read a symphotic pattern in the storage medium and cause the dipole controls to modify one or more dipole values of one or more dipole elements based on the symphotic pattern read from the storage medium.

31. The structure of claim 30 configured for use as one of: a hyperspectral imaging device, encryption algorithms, machine vision, distributed learning, and chemical detection.

32. The structure of claim 30, further comprising an imaging sensor to receive the output object waves as processed image information.

33. The structure of any of claims 30-32, further comprising:

an array of varactor-loaded resonators in communication with the dipole structures; and

bias lines for driving the varactors for dynamic reconfiguration of the three-dimensional array.

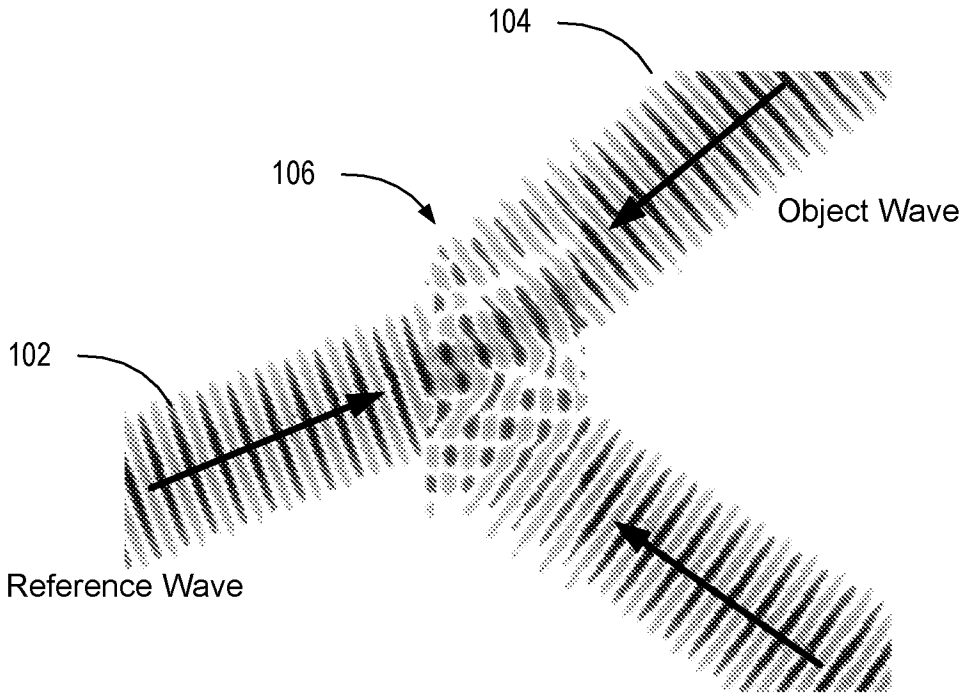

104
106
Object Wave
102
Reference Wave

FIG. 1A

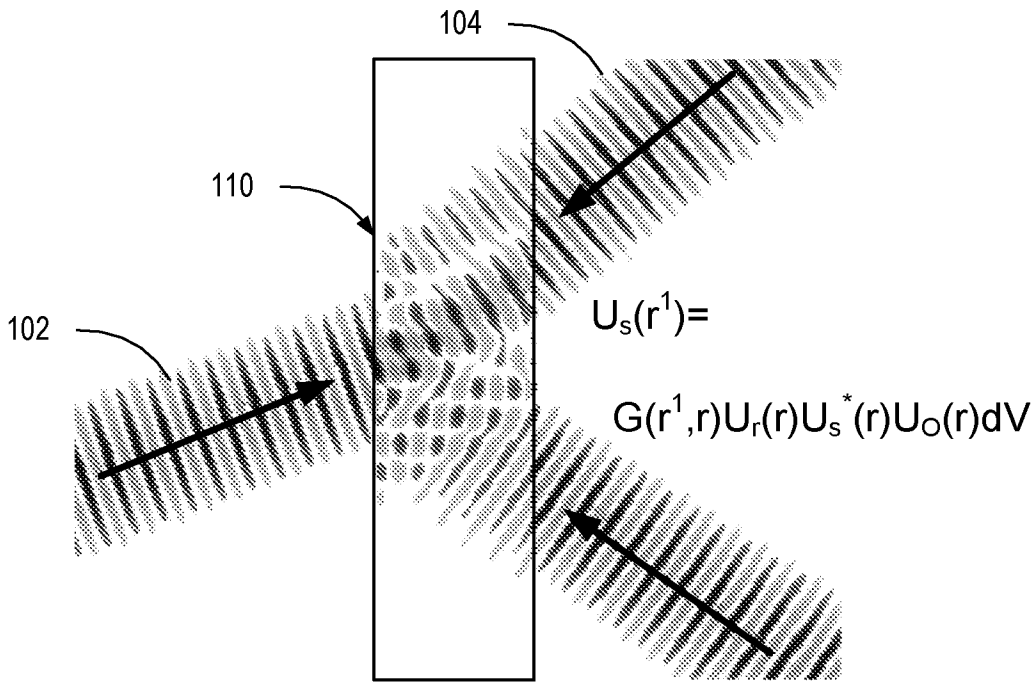

104
110
102
$U_s(r^1)=$
$G(r^1,r)U_r(r)U_s^*(r)U_O(r)dV$

FIG. 1B

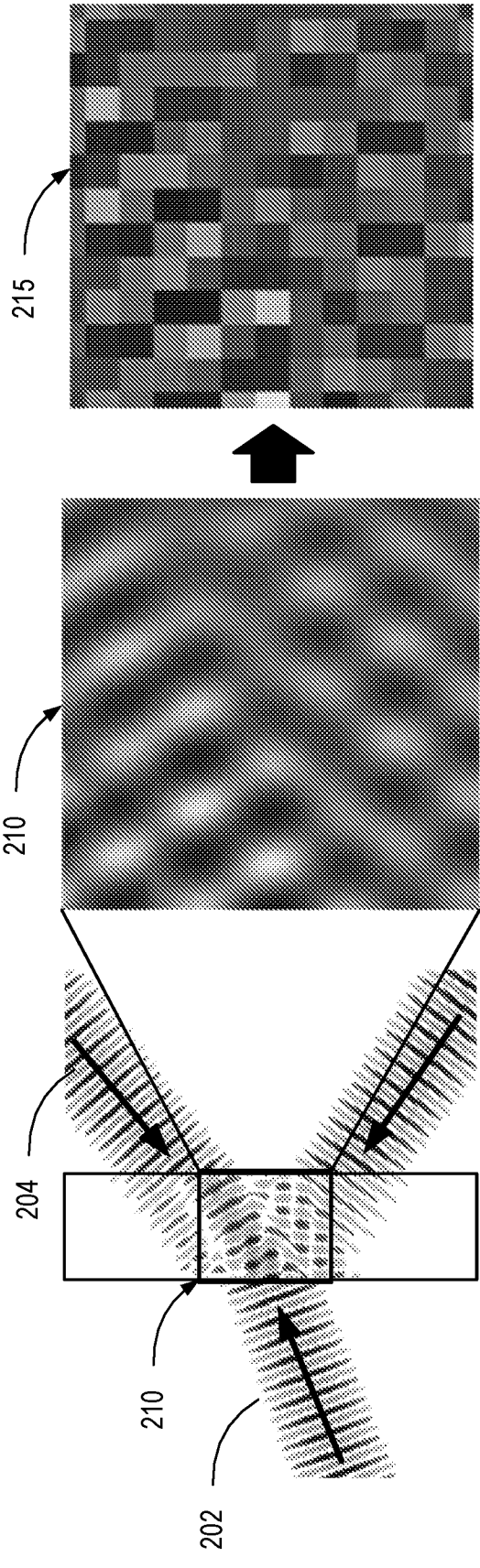


FIG. 2C

FIG. 2B

FIG. 2A

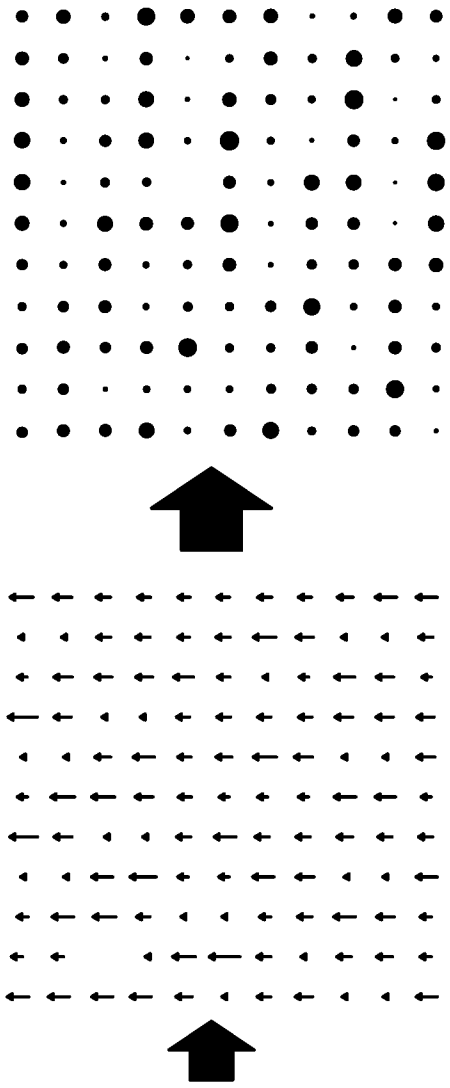


FIG. 2E

FIG. 2D

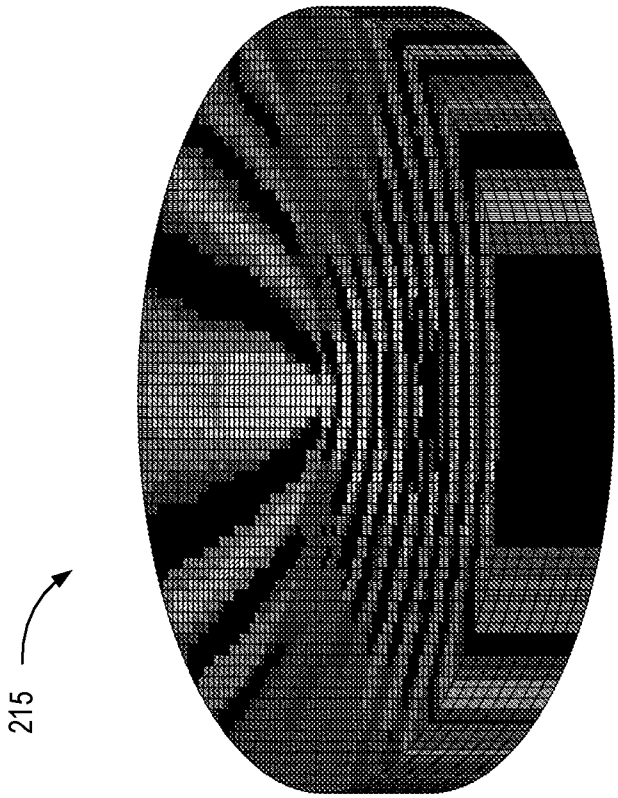


FIG. 2G

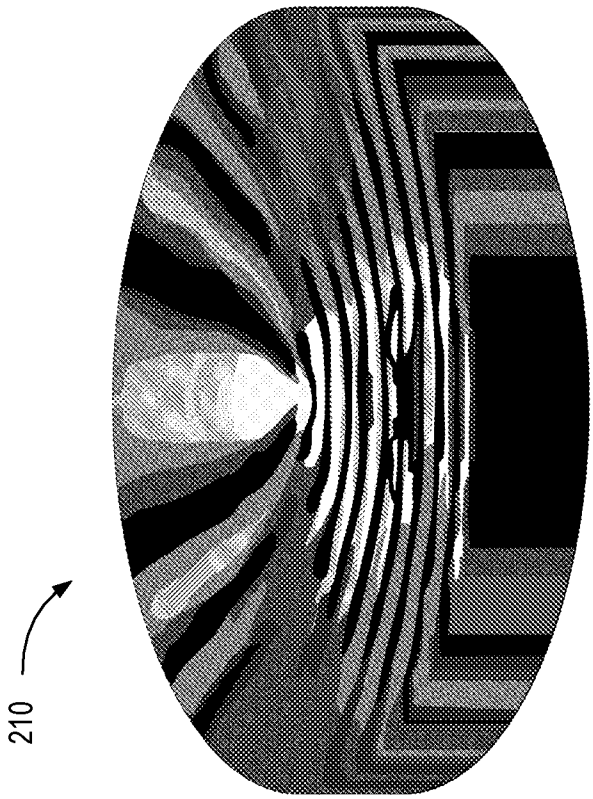


FIG. 2F

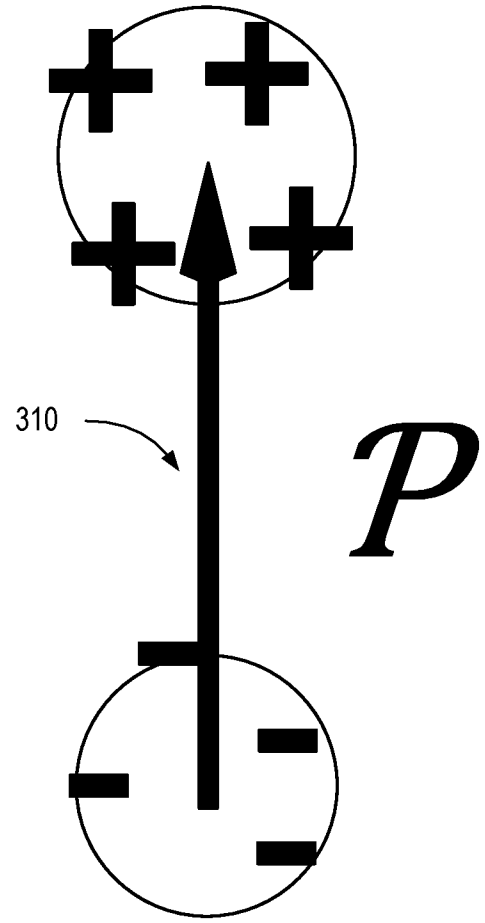


FIG. 3

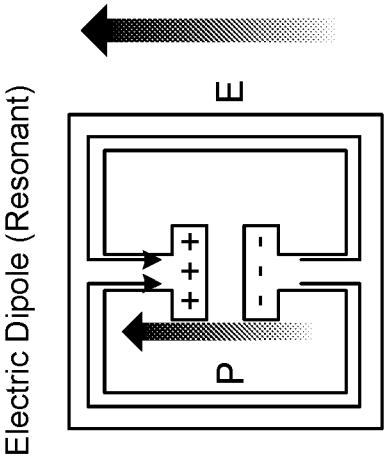


FIG. 4C

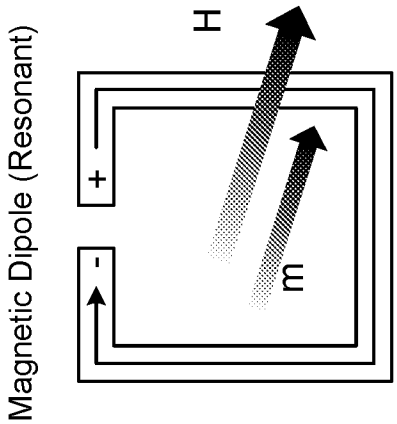


FIG. 4B

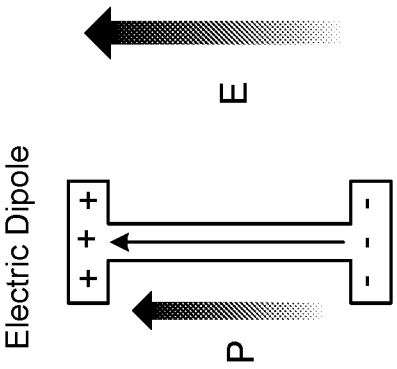


FIG. 4A

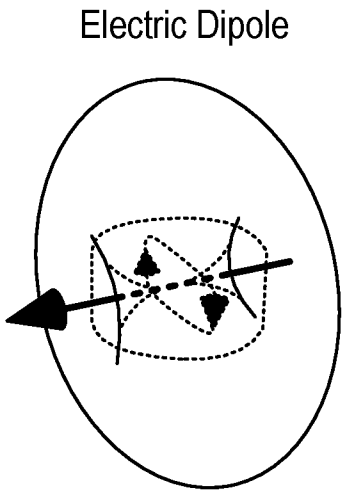
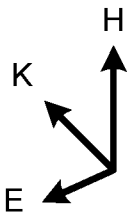


FIG. 5A



E = Electric Field
H = Magnetic Field
K = Incidence

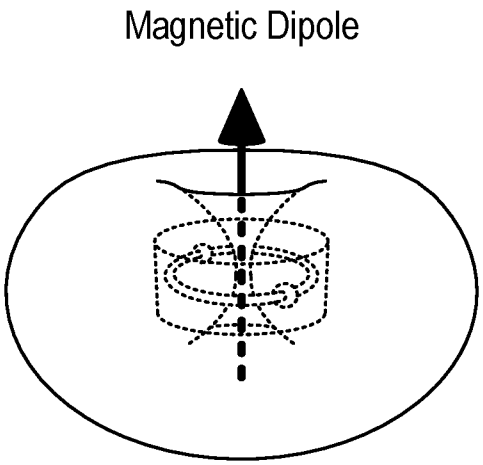


FIG. 5B

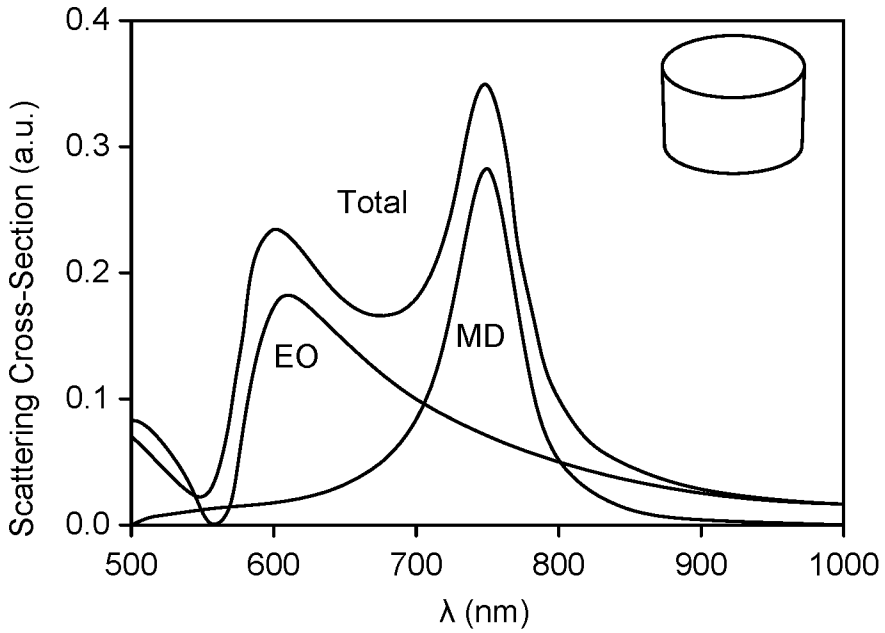


FIG. 5C

Material	Spectral Range, μm	Refractive Index, n
c-Si	0.50-1.45	4.293-3.486
	1.45-2.40	3.484-3.437
a-Si	0.50-1.00	4.47-3.61
GaAs	0.50-0.80	4.037-3.679
GaP	0.50-0.80	3.590-3.197
InP	0.50-0.80	3.456-3.818
TiO_2	0.50-1.00	2.715-2.483
Ge	0.50-0.60	4.460-5.811
	0.60-0.80	5.811-4.699
	0.80-1.90	4.684-4.129
	1.90-2.40	4.111-4.069
GaSb	1.00-2.40	4.140-3.846
Te	4.00-14.0	4.929-4.785
PbTe	4.10-12.5	5.975-5.609
GeTe	6.20-11.8	7.3-7.278
SiC	11.0-15.0	~20

FIG. 6

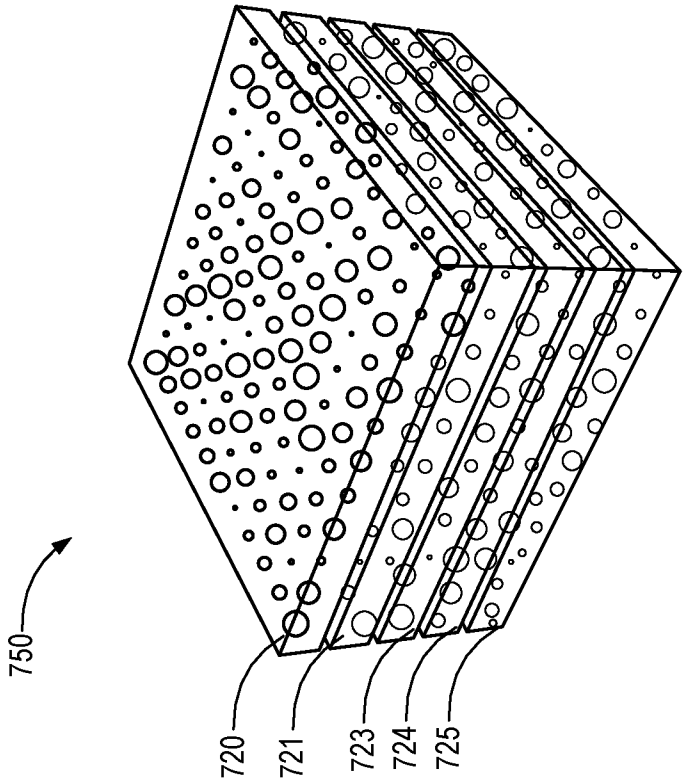


FIG. 7B

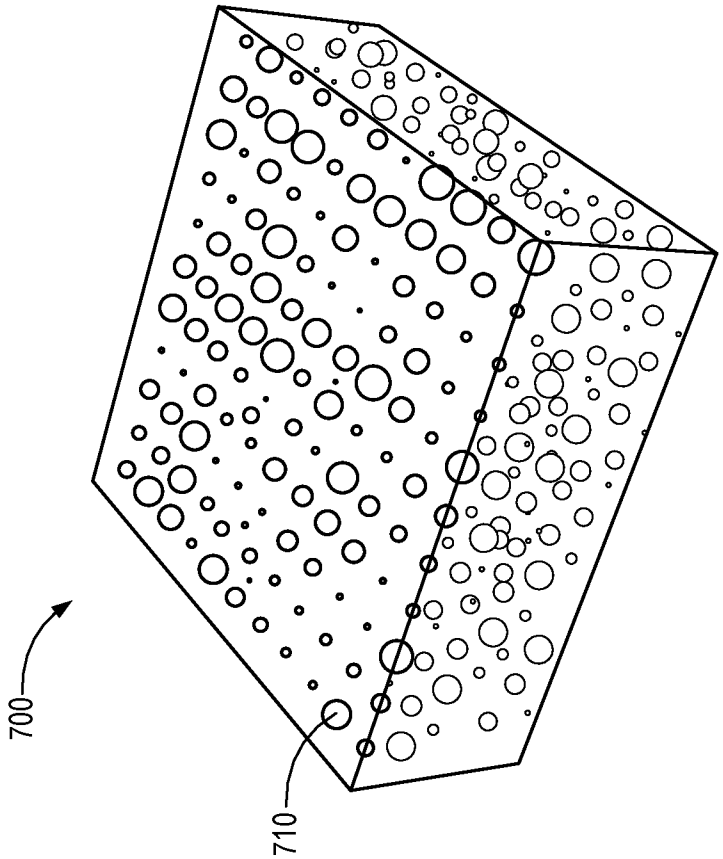


FIG. 7A

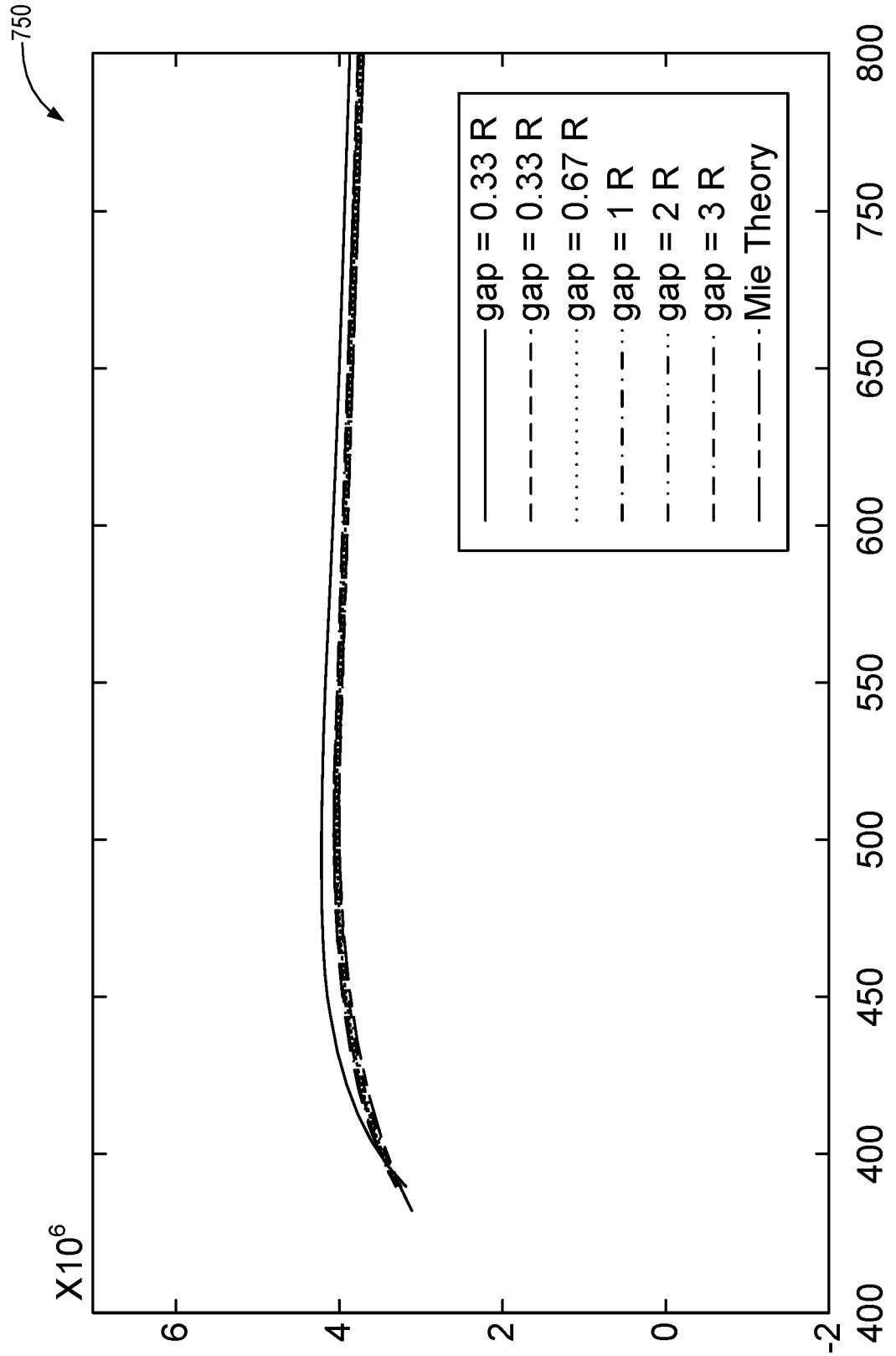

750
X10^6
6
4
2
0
-2
400
450
500
550
600
650
750
800
gap = 0.33 R
gap = 0.33 R
gap = 0.67 R
gap = 1 R
gap = 2 R
gap = 3 R
Mie Theory

FIG. 8

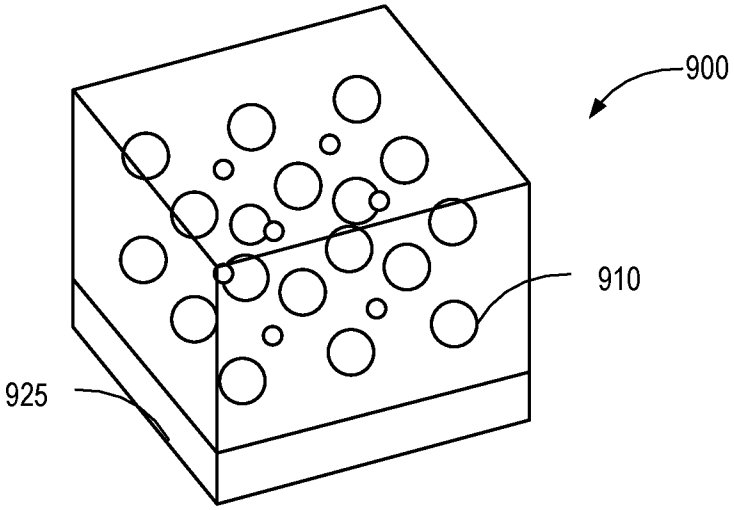


FIG. 9

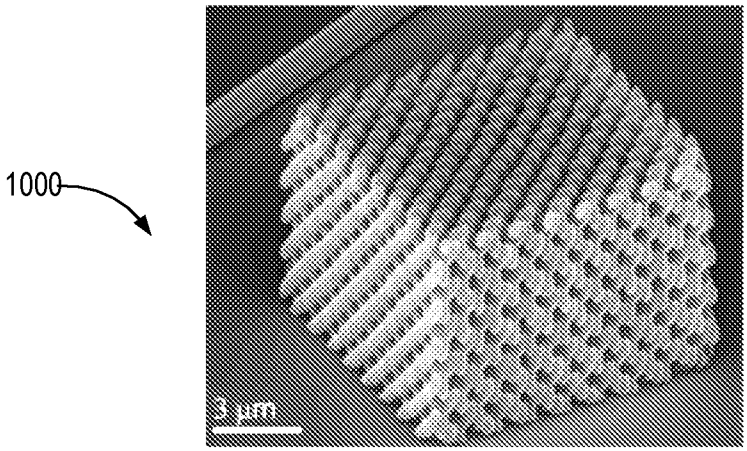


FIG. 10

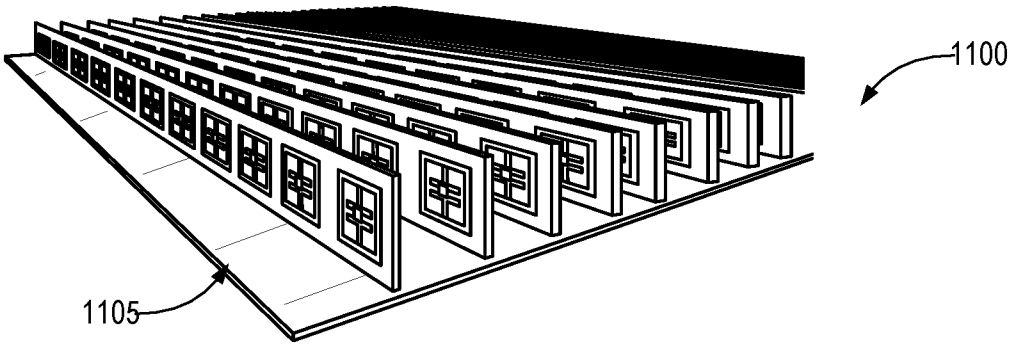


FIG. 11

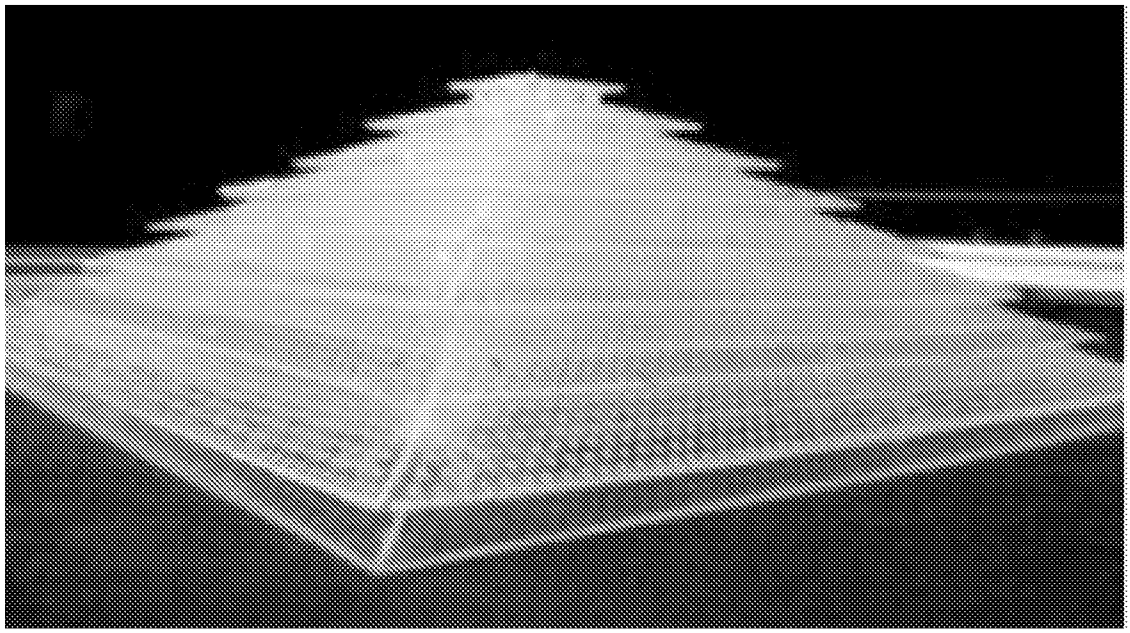


FIG. 12

INTERNATIONAL SEARCH REPORT

International application No.
PCT/US2018/052321

Box No. II Observations where certain claims were found unsearchable (Continuation of item 2 of first sheet)

This international search report has not been established in respect of certain claims under Article 17(2)(a) for the following reasons:

1. ☐ Claims Nos.:
because they relate to subject matter not required to be searched by this Authority, namely:

2. ☒ Claims Nos.: 7-11,28
because they relate to parts of the international application that do not comply with the prescribed requirements to such an extent that no meaningful international search can be carried out, specifically:
Claims 7-11,28 are regarded to be unclear because the claims refer to multiple dependent claims which do not comply with PCT Rule 6.4(a).

3. ☒ Claims Nos.: 6,12-13,15,22-24,27
because they are dependent claims and are not drafted in accordance with the second and third sentences of Rule 6.4(a).

Box No. III Observations where unity of invention is lacking (Continuation of item 3 of first sheet)

This International Searching Authority found multiple inventions in this international application, as follows:

1. ☐ As all required addtional search fees were timely paid by the applicant, this international search report covers all searchable claims.

2. ☐ As all searchable claims could be searched without effort justifying an additional fees, this Authority did not invite payment of any additional fees.

3. ☐ As only some of the required additional search fees were timely paid by the applicant, this international search report covers only those claims for which fees were paid, specifically claims Nos.:

4. ☐ No required additional search fees were timely paid by the applicant. Consequently, this international search report is restricted to the invention first mentioned in the claims; it is covered by claims Nos.:

Remark on Protest

☐ The additional search fees were accompanied by the applicant's protest and, where applicable, the payment of a protest fee.

☐ The additional search fees were accompanied by the applicant's protest but the applicable protest fee was not paid within the time limit specified in the invitation.

☐ No protest accompanied the payment of additional search fees.

INTERNATIONAL SEARCH REPORT

International application No.
PCT/US2018/052321

A. CLASSIFICATION OF SUBJECT MATTER

H01Q 15/10(2006.01)i, H01Q 21/06(2006.01)i

According to International Patent Classification (IPC) or to both national classification and IPC

B. FIELDS SEARCHED

Minimum documentation searched (classification system followed by classification symbols)
H01Q 15/10; C09K 19/18; G01S 13/89; G06F 17/14; H01Q 21/00; H01Q 21/06; H01Q 25/00; H01Q 3/26; H01Q 3/44

Documentation searched other than minimum documentation to the extent that such documents are included in the fields searched
Korean utility models and applications for utility models
Japanese utility models and applications for utility models

Electronic data base consulted during the international search (name of data base and, where practicable, search terms used)
eKOMPASS(KIPO internal) & Keywords: symphotic, dipole, pattern, array, wave

C. DOCUMENTS CONSIDERED TO BE RELEVANT

Category*	Citation of document, with indication, where appropriate, of the relevant passages	Relevant to claim No.
A	US 2015-0333412 A1 (AGENCE SPATIALE EUROPEENNE) 19 November 2015 See paragraphs [0141],[0194]-[0210], claims 1-2 and figures 2A-2D,30.	1-5,14,16-21,25-26,29-33
A	US 2016-0233588 A1 (ADAM BILY et al.) 11 August 2016 See paragraphs [0078],[0084],[0099],[0109] and claim 2.	1-5,14,16-21,25-26,29-33
A	US 2017-0003389 A1 (DUKE UNIVERSITY) 05 January 2017 See paragraph [0136] and figure 4.	1-5,14,16-21,25-26,29-33
A	US 2017-0170557 A1 (KYMETA CORPORATION) 15 June 2017 See paragraphs [0072]-[0073] and figure 10.	1-5,14,16-21,25-26,29-33
A	JP 2009-543394 A (ITI SCOTLAND LTD.) 03 December 2009 See claims 1-4 and figures 2-4.	1-5,14,16-21,25-26,29-33

☐ Further documents are listed in the continuation of Box C.

☒ See patent family annex.

* Special categories of cited documents:
"A" document defining the general state of the art which is not considered to be of particular relevance
"E" earlier application or patent but published on or after the international filing date
"L" document which may throw doubts on priority claim(s) or which is cited to establish the publication date of another citation or other special reason (as specified)
"O" document referring to an oral disclosure, use, exhibition or other means
"P" document published prior to the international filing date but later than the priority date claimed
"T" later document published after the international filing date or priority date and not in conflict with the application but cited to understand the principle or theory underlying the invention
"X" document of particular relevance; the claimed invention cannot be considered novel or cannot be considered to involve an inventive step when the document is taken alone
"Y" document of particular relevance; the claimed invention cannot be considered to involve an inventive step when the document is combined with one or more other such documents,such combination being obvious to a person skilled in the art
"&" document member of the same patent family

Date of the actual completion of the international search	Date of mailing of the international search report
14 January 2019 (14.01.2019)	**14 January 2019 (14.01.2019)**

Name and mailing address of the ISA/KR
International Application Division
Korean Intellectual Property Office
189 Cheongsa-ro, Seo-gu, Daejeon, 35208, Republic of Korea
Facsimile No. +82-42-481-8578

Authorized officer
JANG, Gijeong
Telephone No. +82-42-481-8364

INTERNATIONAL SEARCH REPORT

Information on patent family members

International application No.
PCT/US2018/052321

Patent document cited in search report	Publication date	Patent family member(s)	Publication date
US 2015-0333412 A1	19/11/2015	EP 2949002 A1	02/12/2015
		WO 2014-114993 A1	31/07/2014
US 2016-0233588 A1	11/08/2016	CN 107408761 A	28/11/2017
		EP 3257107 A1	20/12/2017
		JP 2018-505625 A	22/02/2018
		KR 10-2017-0116097 A	18/10/2017
		TW 201719976 A	01/06/2017
		US 2018-0131103 A1	10/05/2018
		US 9893435 B2	13/02/2018
		WO 2016-130383 A1	18/08/2016
US 2017-0003389 A1	05/01/2017	CN 104584326 A	29/04/2015
		CN 104584326 B	08/03/2017
		CN 107015220 A	04/08/2017
		EP 2847823 A2	18/03/2015
		IL 235536 A	29/01/2015
		IN 10174DEN2014 A	21/08/2015
		KR 10-2015-0042746 A	21/04/2015
		US 10109080 B2	23/10/2018
		US 2013-0335256 A1	19/12/2013
		US 2015-0030256 A1	29/01/2015
		US 2016-0266248 A1	15/09/2016
		US 2016-0314602 A1	27/10/2016
		US 9268016 B2	23/02/2016
		US 9411042 B2	09/08/2016
		WO 2014-025425 A2	13/02/2014
		WO 2014-025425 A3	10/07/2014
		WO 2015-054601 A2	16/04/2015
		WO 2015-054601 A3	04/06/2015
US 2017-0170557 A1	15/06/2017	None	
JP 2009-543394 A	03/12/2009	AU 2007-270964 A1	10/01/2008
		CN 101485043 A	15/07/2009
		EP 2041832 A1	01/04/2009
		GB 2439974 A	16/01/2008
		GB 2439974 B	23/03/2011
		KR 10-2009-0068203 A	25/06/2009
		MX 2009000092 A	23/01/2009
		TW 200805788 A	16/01/2008
		US 2008-0122728 A1	29/05/2008
		US 7705797 B2	27/04/2010
		WO 2008-003991 A1	10/01/2008